GEOMETRIZED VACUUM PHYSICS. PART 8: INERTIAL ELECTROMAGNETISM OF MOVING "PARTICLES"

Mikhail Batanov-Gaukhman[1]

(1) Moscow Aviation Institute (National Research University),
Institute No. 2 "Aircraft and rocket engines and power plants",
st. Volokolamsk highway, 4, Moscow – Russia, 125993
(e-mail: alsignat@yandex.ru)

ABSTRACT

This article is the eighth part of the scientific project under the general title "Geometrized Vacuum Physics Based on the Algebra of Signature" [1,2,3,4,5,6,7]. In this article, are proposed metric-dynamic models of "electron" and "positron", which move with constant speed relative to vacuum, stable curvatures of which they themselves are. It is shown that the obtained results are applicable to all "baryons" and "mesons" included in the Standard Model of elementary particles. Model concepts of induction of toroidal-helical vortices around the direction of motion of "particles" and "antiparticles" made it possible to give a completely geometrized explanation of such phenomena as the motion of atomic bodies by inertia (without involving the concept of mass), inertial electric current and inertial electromagnetic field. Like the entire project, this research is aimed at a partial implementation of the Clifford-Einstein-Wheeler program of complete geometrization of physics.

Keywords: electron, positron, geometrized physics, geometrodynamics, vacuum, Algebra of signature, vacuum equations, models of moving elementary particles.

BACKGROUND AND INTRODUCTION

This paper is the eighth in a series of articles under the general title "Geometrized Vacuum Physics (GVPh) Based on the Algebra of Signature (SA)". The previous seven articles are listed in the references [1,2,3,4,5,6,7].

The paper [7] presented metric-dynamic models of a free resting "electron" and a free resting "positron" and considered the quasi-stationary interaction between them.

By quasi-stationary interaction was meant the evaluation of the averaged effect of the outer shell of one stationary "particle" (in particular, an "electron" or "positron") on the core of another stationary "particle" depending on the distance between their centers. In this case, the cause of such an effect are accelerated intra-vacuum currents (i.e., subcont and antisubcont flows twisted into spirals) (see §10 in [7]).

Let's remind once again that within the framework of Geometrical Vacuum Physics (GVPh) we do not know whether intra-vacuum subcont-antisubcont currents exist in reality, or whether these accelerated subcont and antisubcont flows are a figment of the imagination, inspired by the mathematical apparatus. However, if we do not connect the zero components of metric tensors with local flows of various layers of $\lambda_{-12,-15}$-vacuum, then it is practically impossible to verbally describe the processes under study. This is not the first time in science, for example, we do not know whether harmonic additive components (i.e. sinusoids and cosine waves) exist inside complex electrical signals, but this does not prevent the successful application of spectral analysis in many branches of radio engineering.

We note another important circumstance: the GVPh does not have the concept of mass (m). Therefore, within the framework of a fully geometrized theory, it is impossible to formulate the concept of force **F** in the Newtonian sense, i.e. as the product of mass and acceleration ($\mathbf{F} = m\mathbf{a}$). In the theory proposed here, if the core of a "particle" moves with acceleration, it is implied that it is not acted upon by some abstract force, but either by an accelerated vacuum flow, or by a gradient of intra-vacuum tension or pressure from the cores of other moving "particles".

This article examines a moving free valence "electron" and a moving free valence "positron". In the previous article [7] it was noted that there are no separately existing "electrons" and "positrons", since they can only arise from a vacuum together and are in constant interaction. However, for simplicity, in this article the motion of these "particles" is examined separately. First, the moving "electron" is studied, and then, by analogy, the moving "positron" is investigated.

Two cases should be distinguished:

1) The motion of an "electron" (or "positron") relative to an outside observer together with a moving vacuum region, of which it is a deformation. In this case, a moving coordinate system must be used, while the shape of the "electron" and the processes inside it must remain unchanged. In other words, in this situation, the metric-dynamic model of the "electron" (or "positron") continues to be determined by the set of metrics-solutions (1) or (11) in [7], but the coordinate system ct, r, θ, ϕ must move relative to a stationary observer. A separate study of such a motion of the "electron" (or "positron") is required to assess whether it leads to any physical consequences. However, in this article we will focus on the second case.

2) The movement of an "electron" (or "positron") relative to a vacuum region, of which it is a stable curvature. In this case, the shape of the "electron" (or "positron") and the processes inside it change, since in this situation the rapidly moving "electron" (or "positron") experiences resistance from the surrounding stationary vacuum.

Before reading this work, it is most productive to first familiarize yourself with the previous articles of this project [1,2,3,4,5,6,7], since the GVPh uses a number of terms and axioms that were introduced in this theory for the first time. Without a full understanding of these concepts, the content of this article will be incomprehensible. To facilitate reading this article, a glossary of the main terms and definitions first introduced in previous articles is provided below.

Glossary

"Vacuum" – see §1 in [1]. By vacuum in the GVPh we mean the Einstein vacuum, i.e. emptiness in which local material objects are absent. We know nothing about the substantiality of emptiness (i.e. the Einstein vacuum), however, some of its properties are reliably known to us: infinity (possibly closed), bottomlessness (there is no limit to deepening), elastic-plasticity (i.e. the ability to bend and return to the original state), constant and ubiquitous variability (i.e. infinite energy saturation), fractality (repeatability of properties and qualities at different levels), continuous-discreteness (i.e. continuity alternates with distinct phase and/or topological transitions), the speed of propagation of wave disturbances in the Einstein vacuum is equal to the speed of light.

“The vacuum balance condition” – (see §1 in [1]) states that if something appears from a vacuum (i.e. emptiness), it is necessarily in a mutually opposite form (for example, convexity-concavity, wave-antiwave, particle-antiparticle, etc.) so that the opposites, on average, completely compensate for each other’s manifestations.

“$\lambda_{m,n}$-vacuum” – (see §1 [1]) from the above it is clear that “vacuum” (emptiness) is an infinitely complex entity that is extremely difficult to sense and define. Therefore, within the framework of the GVPh it is proposed: on the one hand, to apply analysis as a philosophical method of cognition, i.e. to break down the vacuum, as an infinitely complex entity, into an infinite number of less complex components, and to study them separately; on the other hand, to objectify the subject of study, i.e. to study what can be observed at an acceptable level of reliability. The application of these two general scientific methodological techniques is realized through the introduction of the concept of $\lambda_{m,n}$-vacuum. If we simultaneously probe a certain area of vacuum from three mutually perpendicular directions with monochromatic light beams with a wavelength $\lambda_{m,n}$ from the wavelength range $\Delta\lambda = 10^m - 10^n$ cm (in particular, laser beams, see Figure 1*a* in [1]), we will obtain a light cubic lattice, which can be interpreted as a 3-dimensional light landscape. This 3D light landscape in the GPV is conventionally called the $\lambda_{m,n}$-vacuum. Thus, the $\lambda_{m,n}$-vacuum is a 3-dimensional space that is illuminated from the void by mutually perpendicular light beams with a wavelength of $\lambda_{m,n}$. If the vacuum in a given region is distorted, with curvatures approximately an order of magnitude greater than the wavelength of the probing beams, then the 3-dimensional landscape (i.e. the $\lambda_{m,n}$-vacuum) will also be curved (see Figure 4 in [1]). In this case, the light rays are geodesics of this curved 3-dimensional landscape. It may be objected that light rays are not visible in a vacuum, so no 3D landscape (i.e., $\lambda_{m,n}$-vacuum) is visible. However, the vacuum region under study can be filled with a sol (i.e., a suspension of particles approximately an order of magnitude smaller than the wavelength $\lambda_{m,n}$ of the probing rays), then the 3D light landscape becomes visible (see Figure 1*a* in [1]). One could object to this that a void filled with sol is not a vacuum. Yes, but if the sol particles are significantly smaller than the curvatures of the void, then the distortions introduced by the particles will be insignificant, while larger-scale curvatures of the vacuum are clearly visible as $\lambda_{m,n}$-vacuum. In addition, specialists know that using the radar method, it is possible to determine the curvature of a local section of vacuum without injecting sol. There are also other ways of measuring the curvature of light rays in distorted space. For example, during the eclipse of 1919, the Eddington expedition observed the deflection of a light ray from a star located on the limb of the Sun. If we probe the same area of emptiness with rays of other wavelengths $\lambda_{m+i,n+j}$, in this way, we will obtain an infinite number of $\lambda_{m,n}$-vacuums nested one inside the other (see Figs. 2 and 4 in [1]). All these $\lambda_{m,n}$-vacuums are obey the same laws, but at the same time they all highlight different 3D landscapes, since the diameter of the light rays (i.e. eikonals) depends on their wavelength $\lambda_{m,n}$ (see Fig. 3 in [1]), and the vacuum fluctuations are averaged within the thickness of the probing beam. The decomposition of the "vacuum" into an infinite number of $\lambda_{m,n}$-vacuums in the GPV is called its longitudinal stratification. At the same time, each $\lambda_{m,n}$-vacuum splits into an infinite number of metric spaces and subspaces with 16 types of signatures (i.e. with 16 types of topologies). The description of one of the $\lambda_{m,n}$-vacuums is devoted to the articles [1,2,3,4]. Such a splitting of each $\lambda_{m,n}$-vacuum in the GVPh is called a transverse bundle of the "vacuum". Thus, the "vacuum" is an extremely complex structure consisting of an infinite number of intertwined transverse and longitudinal layers.

"$\boldsymbol{\lambda_{-12,-15}}$**-вакуум**" is a 3D$_{-12,-15}$-landscape illuminated from a "vacuum" by mutually perpendicular light beams with a wavelength of $\lambda_{-12,-15}$ from the range $\Delta\lambda = 10^{-12} \div 10^{-15}$ cm. In articles [5,6,7] and in this article, the greatest attention is paid to this $\lambda_{-12,-15}$-vacuum, since in such a curved 3D$_{-12,-15}$-landscape, the averaged contours of elementary "particles" are clearly visible: "quarks", "leptons", "baryons", "mesons", "atoms", etc. (see articles [6,7]). This longitudinal layer of "vacuum" has been studied most fully, therefore GVPh begins demonstrating the possibilities of stochastic differential geometry and the Algebra of signature precisely with the consideration of metric-dynamic models of elementary "particles". However, as shown in the article [6], in the infinite thickness of "vacuum" there are discrete levels that are fractally similar to each other. Therefore, studying on average stable spherical formations in $\lambda_{-12,-15}$-vacuum, we, in addition, obtain certain knowledge about the average structure of stable spherical vacuum formations in $\lambda_{7,10}$-vacuum (i.e. about "planets" and "stars") and in $\lambda_{17,20}$-vacuum (i.e. about "galaxies"), etc.

"Subcont" and "antisubcont" (see §7 in [2] and §4 in [3]) – as already noted, each $\lambda_{m,n}$-vacuum splits into an infinite number of metric spaces and subspaces with 16 types of signatures (i.e. with 16 types of topologies). However, in the Algebra of signature it is shown that these spaces are superimposed on each other (i.e. added or averaged) in such a way that at the first step (i.e. the zero level of consideration) they completely compensate each other's manifestations, i.e. their sum (or averaging) is zero (see the ranking Ex. (38) in [2]) – this is the expression of the properties of the "vacuum" (bottomless emptiness). At the second step (i.e. at the two-sided level of consideration) the metric spaces are summed (or averaged) in such a way (see §7 in [2]) that from the "vacuum" a 2^3-$\lambda_{m,n}$-vacuum is revealed, which has two adjacent sides: 1) the Minkowski 4-space with the signature (+ – – –), conventionally called the outer side of the $\lambda_{m,n}$-vacuum (or, for brevity and clarity, subcont); 2) the Minkowski 4-antispace with the opposite signature (– + + +), conventionally called the inner side of the $\lambda_{m,n}$-vacuum (or, for brevity and clarity, antisubcont). The concepts of subcont (short for "substantial continuum") and antisubcont (short for "antisubstantial continuum") are speculative and auxiliary. They create the illusion of intertwined elastic-plastic continuous media (conditionally white and black, §4 in [3]) and are intended mainly to visualize and verbally describe the studied intra-vacuum processes at the second level of consideration.

The "substrate" of a stable vacuum formation is a model of the metric-dynamic state of one of the sides of the $\lambda_{m,n}$-vacuum before deformations arose in this region. That is, the substrate is a kind of memory of the "vacuum" about the initial state of some of its regions, with which the deformed state of the same region is compared.

Valence "particle" (in particular, valence "electron" or "positron") - the concept, for example, valence "electron" was introduced in §5 in [7]. In the framework of the GVPh, the "electron" is an infinitely complex stable spherical vacuum formation. However, this is a stepwise complexity that can be regulated by averaging and fixing the level of consideration. The simplest of all possible levels of consideration is called the valence "electron" (or "positron", or "quark", or "proton", or "neutron", etc.).

The principle of "Fair distribution" - this fundamental principle is introduced in §1.5 in [5]. This principle, as applied to the GPhV in a broad sense, means that it is necessary to take into account all solutions of mathematical equations. In a narrow sense, this principle says that it is necessary to take into account all possible metric solutions of the Einstein vacuum equations obtained under the same conditions. The GVPh proposes two main methods for taking into account all similar metric solutions: 1) arithmetic averaging of the components of the metric tensor with the same indices when determining local deformations of the "vacuum"; 2) root-mean-square averaging when determining the acceleration of intertwined intra-vacuum currents (flows) of the "vacuum".

Atomistic body – as noted in §4.13 in [6], an atomistic body in the GVPh is understood to be a dense mixed union of “particles” and “antiparticles” (in particular, “electrons” and “positrons”, “protons” and “antiprotons”, “neutrons”, etc.). Baryon asymmetry of matter is absent in this hypothesis. The reason that “particles” and “antiparticles” in an atomistic body do not annihilate is presumably related to their complex (topological, or nodal) interweaving, mixing, and constant participation in thermal (chaotic) motion (i.e. the presence of conserved inertia of motion and rotation).

MATERIALS AND METHOD

1 Uniform and rectilinear motion of a free “electron” relative to a stationary vacuum

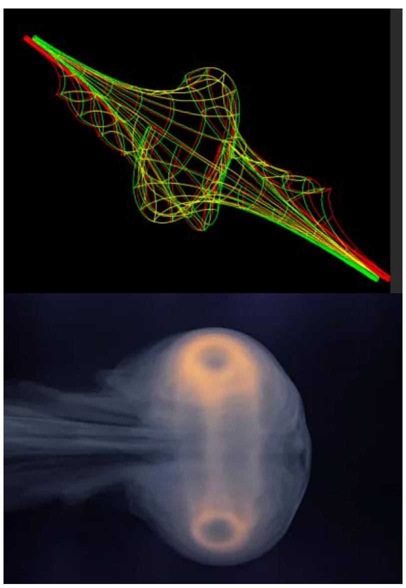

Fig. 1. Schematic representation of a soliton and the translational motion of a toroidal vortex (toroid) in a gaseous medium

The motion of stable local disturbances in liquid and gaseous media, of which they themselves consist, is of two types (Figure 1):
1) self-consistent solitons;
2) toroidal vortices.

A moving "electron" has a combination of properties of a soliton and a rotating toroid. Firstly, a stationary "electron" is a self-consistent soliton in which the deformations of the $\lambda_{-12,-15}$-vacuum are maintained by accelerated subcont flows [7]. Secondly, by analogy with similar natural processes, the motion of the "electron" core should entrain the surrounding $\lambda_{-12,-15}$-vacuum into a toroidal rotational motion (Figure 2).

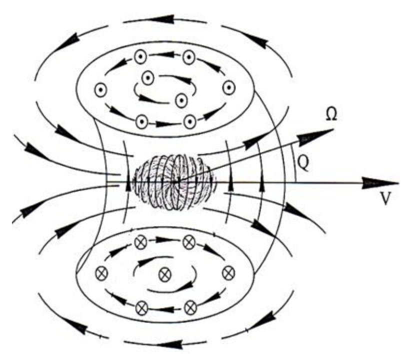

Fig. 2. Schematic representation of the motion of an “electron” in a $\lambda_{-12,-15}$- vacuum, of which it is a deformation

That is, it is expected that with the rectilinear uniform motion of a free "electron", relative to the $\lambda_{-12,-15}$-vacuum of which it itself consists, its outer shell and core should rotate around an axis that itself precesses (rotates) around the direction of motion. In this case, it is expected that the outer shell of the "electron" takes the form of a toroidal vortex (toroid), moving in the direction of the Z axis, and the core should take the form of an elongated ellipsoid (see Figure 2)

$$\frac{x^2}{r_q^2(1-V_z^2/V_{\max}^2)}+\frac{y^2}{r_q^2(1-V_z^2/V_{\max}^2)}+\frac{z^2}{r_q^2}=1, \tag{1}$$

where

r_q is the radius of the initial sphere,

V_z is the velocity of the ellipsoid in the direction of the *Z* axis,

V_{max} is the velocity of propagation of disturbances in the medium of which this toroid consists. In particular, for a vacuum this velocity is equal to the speed of light ($V_{max} = c$).

2 Outer shell of a moving free "electron"

2.1 Ellipticity parameter

Let's consider a simplified case where the outer shell of a uniformly and rectilinearly moving "electron" rotates around an axis that does not precess around the direction of its motion. We assume that in this model representation the outer shell of a moving "electron" is described not by the Schwarzschild metrics (24) and (25) in [7], but by the corresponding Kerr metrics in Boyer-Lindquist coordinates

for the *a*-subcont:

$$ds_1^{(+a)2}=\left(1-\frac{r_6r}{\rho^{(+a)}}\right)c^2dt^2-\frac{\rho^{(+a)2}dr^2}{\Delta^{(+a)}}-\rho^{(+a)}d\theta^2-\left(r^2+a_a^2+\frac{r_6ra_a^2}{\rho^{(+a)}}sin^2\,\theta\right)sin^2\,\theta\,d\phi^2+\frac{2r_6ra_a}{\rho^{(+a)}}sin^2\,\theta\,cdtd\phi, \tag{2}$$

where $\rho^{(+a)} = r^2 + a_a^2 cos^2\theta$, $\Delta^{(+a)} = r^2 + a_a{}^2 - r_6 r$;

for the *b* -subcont:

$$ds_2^{(+b)2}=\left(1+\frac{r_6r}{\rho^{(+b)}}\right)c^2dt^2-\frac{\rho^{(+b)2}dr^2}{\Delta^{(+b)}}-\rho^{(+b)}d\theta^2-\left(r^2+a_b^2-\frac{r_6ra_b^2}{\rho^{(+b)}}sin^2\,\theta\right)sin^2\,\theta\,d\phi^2-\frac{2r_6ra_b}{\rho^{(+b)}}sin^2\,\theta\,cdtd\phi, \tag{3}$$

where $\rho^{(+b)} = r^2 + a_b{}^2\cos^2\theta$, $\Delta^{(+b)} = r^2 + a_b{}^2 + r_6 r$,

a_a is the ellipticity parameter for the *a*-subcont (see below),

a_b is the ellipticity parameter for the *b*-subcont.

Metrics (2) and (3) are exact solutions of the Einstein vacuum equation (42) in [5] ($R_{ik} = 0$) for the case of a constantly rotating stable spherical vacuum formation. These metrics-solutions were discovered by Roy Kerr in 1963 [4], but in the form (2) they were first given by Boyer and Lindquist in 1967.

The metric (3), defining the metric-dynamic state of the *b*-subcont, is obtained by replacing all r_6 with $-r_6$ in the metric (2), defining the metric-dynamic state of the *a*-subcont (just as the metric (25) in [7] is obtained from the metric (24) in [7]).

The radius r6 is taken from the discrete hierarchy of radii (44a) in [6].
For ellipticity parameters $a_a = a_b = 0$, the Kerr metrics (2) and (3) transform into the Schwarzschild metrics (24) and (25) in [7], respectively, and for $r_6 = 0$, these metrics become Galilean:

$$ds_1^{(+a)2}=c^2dt^2-\frac{\rho^{(+a)}dr^2}{r^2+a_a^2}-\rho^{(+a)}d\theta^2-(r^2+a_a^2)\,sin^2\,\theta\,d\phi^2, \tag{4}$$

$$ds_2^{(+b)2}=c^2dt^2-\frac{\rho^{(-b)}dr^2}{r^2+a_b^2}-\rho^{(+b)}d\theta^2-(r^2+a_b^2)\,sin^2\,\theta\,d\phi^2. \tag{5}$$

Let's demonstrate this using the metric as an example. For example, the metric (4) is indeed Galilean

$ds^2 = c^2dt^2 - dx^2 - dy^2 - dz^2$, (6)

in spatially flattened coordinates. To demonstrate this, we introduce the coordinates

$$x = \sqrt{r^2 + a_a^2}\, sin\,\theta\, cos\,\phi, \quad (7)$$
$$y = \sqrt{r^2 + a_a^2}\, sin\,\theta\, sin\,\phi,$$
$$z = r\, cos\,\theta.$$

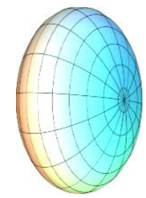

In these coordinates, the metric (4) takes the form of the Galilean metric (6). In this case, the surfaces r = const are oblate ellipsoids of revolution, described by the equation

$$\frac{x^2}{r^2+a_a^2} + \frac{y^2}{r^2+a_a^2} + \frac{z^2}{r^2} = 1. \quad (8)$$

Comparing Exs. (1) and (8), we find that the parameter aa, which determines the degree of ellipticity of a moving stable subcont formation, can be determined as follows:

$$a_a = \pm r_q \frac{V_z}{c}, \quad (9)$$

let's call it the a-subcont ellipticity parameter.

Similarly, for the metric (3), which describes the behavior of the b-subcont, we obtain the b-subcont ellipticity parameter

$$a_b = \mp r_q \frac{V_z}{c}. \quad (11)$$

On the other hand, the ellipticity parameters aa and ab can be determined from the following considerations.

The component g_{11}, for example, of the metric (2) becomes infinite at $\Delta^{(+a)} = r^2 + a_a^2 - r_6 r = 0$, from which we find the radius of the a-subcont horizon [8]

$$r_0 = \frac{r_6}{2} \pm \sqrt{\left(\frac{r_6}{2}\right)^2 - a_a^2}. \quad (12)$$

In turn, the component g_{00} of the same metric (2) vanishes at $\rho^{(+a)\,2} = r^2 + a_a^2\cos^2\theta = r_6\, r$, from this expression we can determine the radius of the surface of infinite redshift [8]

$$r_s = \frac{r_6}{2} \pm \sqrt{\left(\frac{r_6}{2}\right)^2 - a_a^2\, cos^2\,\theta}. \quad (13)$$

From Exs. (12) and (13) it follows that the subcont ellipticity parameter a_a cannot exceed the limiting value [8]

$$a_{a\,max} = \frac{r_6}{2}. \quad (14)$$

According to Ex. (9), the maximum value of the parameter a_a is achieved at $V_z = c$. In this case, when comparing Exs. (9) and (14), we obtain the correspondence $r_q \equiv \frac{r_6}{2}$. This allows us to finally determine the values of the ellipticity parameters

$$a_a = \pm \frac{r_6 V_z}{2c} = \pm \frac{r_6^2 \omega_z}{2c} \quad \text{– for the } a\text{-subcont}, \quad (15)$$

$$a_b = \mp \frac{r_6 V_z}{2c} = \mp \frac{r_6^2 \omega_z}{2c} \quad \text{– for the } b\text{-subcont}, \quad (16)$$

where $\omega_z = \frac{V_z}{r_6}$ is the angular velocity of rotation of a sphere with radius r_6. (17)

The quantity $L_e = \frac{r_6^2 \omega_z}{2}$ is an analogue of the angular momentum of a solid disk of radius r6 rotating with an angular velocity ω_z. Therefore, the parameters of *a*-subcont and *b*-subcont ellipticity can be represented as

$a_a = \pm \frac{L_e}{c}$ and $a_b = \mp \frac{L_e}{c}$.

2.2 Metric-dynamic model of the outer shell of a moving free "electron"

The above analysis, taking into account the principle of "Fair distribution" (see §1.5 in [5]), allows us to propose the following most complete set of Kerr metrics-solutions to the Einstein vacuum equation for constructing a metric-dynamic model of the outer shell of a free valence "electron" that moves rectilinearly and uniformly (i.e. with a constant velocity V_z) in a $\lambda_{-12,-15}$-vacuum, of which it is a stable curvature.

"ELECTRON"

moving rectilinearly and uniformly with velocity V_z in the direction of the Z axis

The outer shell of a free valence "electron",
moving rectilinearly and uniformly (Figure 2) (20)

in the interval [r_4, r_6], signature (+ – – –)

I $$ds_1^{(+a1)2} = \left(1 - \frac{r_6 r}{\rho}\right) c^2 dt^2 - \frac{\rho dr^2}{\Delta^{(a)}} - \rho d\theta^2 - \left(r^2 + a^2 + \frac{r_6 r a^2}{\rho} sin^2\,\theta\right) sin^2\,\theta\, d\phi^2 + \frac{2 r_6 r a}{\rho} sin^2\,\theta\, d\phi c dt, \quad (21)$$

H $$ds_2^{(+a2)2} = \left(1 - \frac{r_6 r}{\rho}\right) c^2 dt^2 - \frac{\rho dr^2}{\Delta^{(a)}} - \rho d\theta^2 - \left(r^2 + a^2 + \frac{r_6 r a^2}{\rho} sin^2\,\theta\right) sin^2\,\theta\, d\phi^2 - \frac{2 r_6 r a}{\rho} sin^2\,\theta\, d\phi c dt, \quad (22)$$

V $$ds_3^{(+b1)2} = \left(1 + \frac{r_6 r}{\rho}\right) c^2 dt^2 - \frac{\rho dr^2}{\Delta^{(b)}} - \rho d\theta^2 - \left(r^2 + a^2 - \frac{r_6 r a^2}{\rho} sin^2\,\theta\right) sin^2\,\theta\, d\phi^2 + \frac{2 r_6 r a}{\rho} sin^2\,\theta\, d\phi c dt, \quad (23)$$

H′ $$ds_4^{(+b2)2} = \left(1 + \frac{r_6 r}{\rho}\right) c^2 dt^2 - \frac{\rho dr^2}{\Delta^{(b)}} - \rho d\theta^2 - \left(r^2 + a^2 - \frac{r_6 r a^2}{\rho} sin^2\,\theta\right) sin^2\,\theta\, d\phi^2 - \frac{2 r_6 r a}{\rho} sin^2\,\theta\, d\phi c dt; \quad (24)$$

The substrate of "electron"

uniformly and rectilinearly moving, see metrics (4) and (5),

$r \in [0, \infty]$, signature (+ – – –)

i $$ds_5^{(+)2} = c^2 dt^2 - \frac{\rho dr^2}{r^2 + a^2} - \rho d\theta^2 - (r^2 + a^2)\, sin^2\,\theta\, d\phi^2, \quad (25)$$

where $\rho = r^2 + a^2 cos^2\theta$, $\Delta^{(a)} = r^2 - r_6 r + a^2$, $\Delta^{(b)} = r^2 + r_6 r + a^2$;

$a = \frac{r_6 V_z}{2c}$ is the ellipticity parameter. (25′)

Similarly, we obtain the following completely opposite set of Kerr metric solutions for the metric-dynamic model of the outer shell of a free valence “positron” moving rectilinearly and uniformly with velocity V_z in the direction of the Z axis

"POSITRON"

moving rectilinearly and uniformly with velocity V_z in the direction of the Z axis

The outer shell of a free valence "positron",
moving rectilinearly and uniformly (negative **Figure 2)** (26)

in the interval [r_4, r_6], signature (– + + +)

H′ $$ds_1^{(-a1)2} = -\left(1-\frac{r_6 r}{\rho}\right)c^2dt^2 + \frac{\rho dr^2}{\Delta^{(a)}} + \rho d\theta^2 + \left(r^2+a^2+\frac{r_6 ra^2}{\rho}sin^2\,\theta\right)sin^2\,\theta\,d\phi^2 - \frac{2r_6 ra}{\rho}sin^2\,\theta\,d\phi cdt, \quad (27)$$

V $$ds_2^{(-a2)2} = -\left(1-\frac{r_6 r}{\rho}\right)c^2dt^2 + \frac{\rho dr^2}{\Delta^{(a)}} + \rho d\theta^2 + \left(r^2+a^2+\frac{r_6 ra^2}{\rho}sin^2\,\theta\right)sin^2\,\theta\,d\phi^2 + \frac{2r_6 ra}{\rho}sin^2\,\theta\,d\phi cdt, \quad (28)$$

H $$ds_3^{(-b1)2} = -\left(1+\frac{r_6 r}{\rho}\right)c^2dt^2 + \frac{\rho dr^2}{\Delta^{(b)}} + \rho d\theta^2 + \left(r^2+a^2-\frac{r_6 ra^2}{\rho}sin^2\,\theta\right)sin^2\,\theta\,d\phi^2 - \frac{2r_6 ra}{\rho}sin^2\,\theta\,d\phi cdt, \quad (29)$$

I $$ds_4^{(-b2)2} = -\left(1+\frac{r_6 r}{\rho}\right)c^2dt^2 + \frac{\rho dr^2}{\Delta^{(b)}} + \rho d\theta^2 + \left(r^2+a^2-\frac{r_6 ra^2}{\rho}sin^2\,\theta\right)sin^2\,\theta\,d\phi^2 + \frac{2r_6 ra}{\rho}sin^2\,\theta\,d\phi cdt; \quad (30)$$

The substrate of "positron"

uniformly and rectilinearly moving,

in the interval $r \in [0, \infty]$, signature (– + + +)

i $$ds_5^{(-)2} = -c^2dt^2 + \frac{\rho dr^2}{r^2+a^2} + \rho d\theta^2 + (r^2+a^2)\,sin^2\,\theta\,d\phi^2. \quad (31)$$

The sets of metrics (20) and (26) when added (or averaged) completely compensate each other's manifestation

$$\frac{1}{10}\left(ds_1^{(+a1)2} + ds_2^{(+a2)2} + ds_3^{(+b1)2} + ds_4^{(+b2)2} + ds_5^{(+)2} + ds_1^{(-a1)2} + ds_2^{(-a2)2} + ds_3^{(-b1)2} + ds_4^{(-b2)2} + ds_5^{(-)2}\right) = 0, \quad (32)$$

which corresponds to the vacuum balance condition (see the glossary in the Introduction or §1 in [1]).

All metrics (21) – (25) and (27) – (31) are solutions of the Einstein vacuum equation (i.e., satisfy the conservation condition, see §1 in [5]), which essentially means (as has been noted more than once in [1,2,3,4,5,6,7]) that these solutions describe, on average, stable vacuum formations. Only in this case, on average, stable vacuum formations are not at rest, but move rectilinearly and uniformly with a constant velocity relative to the $\lambda_{-12,-15}$-vacuum of which they themselves consist (i.e., of which they are stable curvatures).

3 Deformations of the outer shell of a free "electron" moving at a constant speed

When constructing metric-dynamic models of the outer shell of a moving "electron" and a moving "positron" based on sets of metrics (21) – (25) and (27) – (31), we use the method described in §2.8 in [5] and applied in §2 in [7]. First, we will consider a moving free "electron", and then apply the obtained results by analogy to the description of a moving free "positron".

We average the metrics (21) – (24), as a result we obtain

$$ds_{12}^{(+)2} = \frac{1}{4}\left(ds_1^{(+a1)2} + ds_2^{(+a2)2} + ds_3^{(+b1)2} + ds_4^{(+b2)2}\right) = g_{00}^{(+)}c^2dt^2 + g_{11}^{(+)}dr^2 + g_{22}^{(+)}d\theta^2 + g_{33}^{(+)}\,sin^2\,\theta\,d\phi^2 + g_{03}^{(+)}d\phi cdt, \quad (33)$$

where

$$g_{00}^{(+)} = \frac{1}{4}\left(g_{00}^{(+a1)} + g_{00}^{(+a2)} + g_{00}^{(+b1)} + g_{00}^{(+b2)}\right) = \frac{1}{2}\left(1-\frac{r_6 r}{\rho} + 1 - \frac{r_6 r}{\rho} + 1 + \frac{r_6 r}{\rho} + 1 + \frac{r_6 r}{\rho}\right) = 1, \quad (34)$$

$$g_{11}^{(+)} = -\frac{1}{4}\left(\frac{\rho}{\Delta^{(a)}} + \frac{\rho}{\Delta^{(a)}} + \frac{\rho}{\Delta^{(b)}} + \frac{\rho}{\Delta^{(b)}}\right) = -\frac{(r^2+a^2cos^2\theta)(r^2+a^2)}{(r^2-r_6 r+a^2)(r^2+r_6 r+a^2)},$$

$$g_{22}^{(+)} = -\frac{1}{4}(\rho+\rho+\rho+\rho) = -\rho = -(r^2+a^2cos^2\theta),$$

$$g_{33}^{(+)} = -\frac{1}{4}\left[2\left(r^2+a^2+\frac{r_6 ra^2\,sin^2\,\theta}{\rho}\right) + 2\left(r^2+a^2-\frac{r_6 ra^2\,sin^2\,\theta}{\rho}\right)\right]sin^2\,\theta = -(r^2+a^2)\,sin^2\,\theta,$$

$$g_{03}^{(+)} = \frac{1}{4}\left(\frac{2r_6 ra}{\rho} - \frac{2r_6 ra}{\rho} + \frac{2r_6 ra}{\rho} - \frac{2r_6 ra}{\rho}\right)sin^2\,\theta = 0,$$

other components $g_{ij}^{(+)} = 0$.

Components of the metric tensor $g_{ij0}^{(+)}$ from the metric of the moving "electron" substrate (25):

$$g_{000}^{(+)} = 1, \quad g_{110}^{(+)} = -\frac{\rho^{(+)}}{r^2+a^2} = -\frac{r^2+a^2cos^2\theta}{r^2+a^2}, \quad g_{220}^{(+)} = -\rho^{(+)} = -(r^2+a^2cos^2\theta), \quad g_{330}^{(+)} = -(r^2+a^2)\, sin^2\theta. \tag{35}$$

Let's consider the deformations of the outer side of the $\lambda_{-12,-15}$-vacuum (i.e. the subcont) arising in the outer shell of a free "electron" moving with a constant velocity V_z in the direction of the Z axis.

We will judge the deformations of the subcont by the relative elongation (47) in [3]

$$l_i^{(+)} = \sqrt{1 + \frac{g_{ii}^{(+)} - g_{iio}^{(+)}}{g_{iio}^{(+)}}} - 1 = \sqrt{\frac{g_{ii}^{(+)}}{g_{iio}^{(+)}}} - 1. \tag{36}$$

Let's substitute components (34) and (35) into the expression for relative elongation (36), and as a result, for three spatial directions we obtain

$$l_r^{(+)} = \frac{\Delta r}{r} = \sqrt{\frac{(r^2+a^2)^2}{(r^2-r_6r+a^2)(r^2+r_6r+a^2)}} - 1, \quad l_\theta^{(+)} = 0, \quad l_\phi^{(+)} = 0, \tag{37}$$

where $a = \frac{r_6V_z}{2c}$ is the ellipticity parameter.

The graph of the relative elongation function of the subcont in the radial direction $l_r^{(+)} = \Delta r/r$ (37) with the conventionally accepted $r_6 = 1$ and V_z/c = 0.007, V_z/c = 0.0007 and V_z/c = 0.00007 is shown in Figure 3. From which it is clear that with a change in the ratio V_z/c (i.e. with a change in the speed of rectilinear and uniform motion of a stable vacuum formation), the deformation of the outer shell relative to its curved substrate does not change.

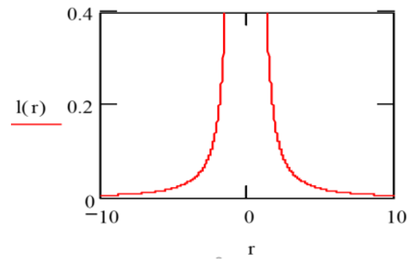

Fig. 3. Graph of the function of relative elongation of the outer side of the $\lambda_{-12,-15}$-vacuum (i.e. subcont) in the outer shell of a moving "electron" in the radial direction (37) $l_r^{(+)} = \Delta r/r$ at $r_6 = 1$ and V_z/c =0.007, V_z/c =0.0007, V_z/c =0.00007

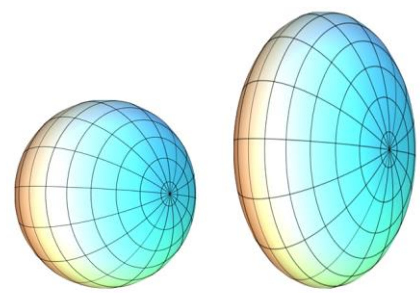

a) b)

Fig. 4. As the velocity V_z of the rectilinear motion of the "electron" increases, the geodesic lines of the "electron" substrate take the form of an increasingly flattened ellipsoid (spheroid) of rotation.

However, with an increase in the speed V_z, the substrate of the moving "electron", according to Exs. (4) – (11), acquires the shape of an increasingly flattened ellipsoid of revolution (Figure 4).

4 Flows in the outer shell of an "electron" and a "positron" moving rectilinearly and uniformly

4.1 Estimation of the velocity of movement of a subcont in the outer shell of a moving "electron"

Let's consider the radial component of the velocity of the a_1-subcont in the outer shell of a moving "electron". To do this, similar to how this was done for the outer shell of a stationary "electron" (see §2.2.1 in [7]), we compare the dynamic metric (38) and the kinematic metric (96) in [3]

$$ds^{(+)2} = \left(1 - \frac{v_r^2}{c^2}\right)c^2dt^2 + 2v_rdrdt - dr^2 - r^2d\theta^2 - r^2sin^2\theta\, d\phi^2, \tag{38}$$

this is more suitable for this case.

We identically equate the zero components $g_{00}^{(+a1)}$ of the metric (38) and g_{00} of the metric (41), assuming that $v_x = v_r^{(+a1)}$

$$\left(1 - \frac{v_r^{(+a1)2}}{c^2}\right) \equiv \left(1 - \frac{r_6 r}{r^2 + a^2 \cos^2\theta}\right).$$

From where we find the heuristic relation

$$\frac{v_r^{(+a1)2}}{c^2} \equiv \frac{r_6 r}{r^2 + a^2 \cos^2\theta}\,. \qquad (39)$$

From which follows the estimated expression for the velocity of the a_1-subcont in the outer shell of the moving "electron"

$$v_r^{(+a1)} \equiv c\sqrt{\frac{r_6 r}{r^2 + a^2 \cos^2\theta}}\,. \qquad (43)$$

Let's consider the tangential component of the velocity of the a_1-subcont in the outer shell of the moving "electron".

In §6.2 in [3] it is shown that if the front and back of the subcont rotate around the *Z* axis in the same direction with the angular velocity of rotation Ω, then this kinematic case is described by the metric (99) in [3] in cylindrical coordinates

$$ct = ct\,, \quad r^2 = x^2 + y^2, \quad z = z, \quad \varphi = \mathrm{arctg}(y/x) - \Omega t,$$

this metric takes the form

$$ds^{(+)2} = \left(1 - \frac{r^2\Omega^2}{c^2}\right)c^2dt^2 - dr^2 - r^2 d\varphi^2 - dz^2 + \frac{2r^2\Omega^2}{c}\,d\varphi c dt. \qquad (41)$$

Comparing the component $g_{03}^{(+a1)}$ in the metric (21) and g_{03} in the metric (41), we find a correspondence

$$\frac{2r^2\Omega}{c} = \frac{2rv_\phi^{(+a1)}}{c} \equiv \frac{r_6 ra}{r^2 + a^2\cos^2\theta}\sin^2\theta, \quad \text{where} \quad \Omega = \frac{v_\phi^{(+a1)}}{r}\,, \qquad (42)$$

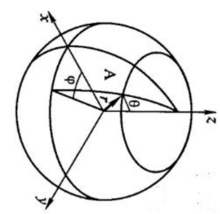

from which we can obtain an estimate of the tangential component of the motion of the a_1-subcont in the outer shell of the moving "electron" moving with velocity V_z in the direction of the *Z* axis

$$v_\phi^{(+a1)} \equiv \frac{cr_6 a}{r^2 + a^2\cos^2\theta}\sin^2\theta. \qquad (43)$$

In the metric (21) there are no components of the metric tensor g_{02} (i.e. $g_{02} = g_{20} = 0$) therefore

$$v_\theta^{(+a1)} \equiv 0. \qquad (44)$$

Thus, we will assume that the velocity vector $\vec{v}^{(+a1)}$ of the a_1-subcont in each local region in the outer shell of the "electron" moving with velocity V_z in the direction of the *Z* axis has components (40), (43), (44)

$$v_r^{(+a1)} \equiv c\sqrt{\frac{r_6 r}{r^2 + a^2\cos^2\theta}}\,, \quad v_\phi^{(+a1)} \equiv \frac{cr_6 a}{r^2 + a^2\cos^2\theta}\sin^2\theta, \quad v_\theta^{(+a1)} \equiv 0. \qquad (45)$$

The velocity component $v_r^{(+a1)}$ of the a_1-subcont is associated with the electrical interaction, and it is very large compared to the velocity component $v_\phi^{(+a1)}$ associated with the magnetic interaction. Therefore, it is not possible to show the total velocity field of the a_1-subcont in one figure. Because of this, Figure 5.1 shows one of the sections of only the velocity field $v_\phi^{(+a1)}$.

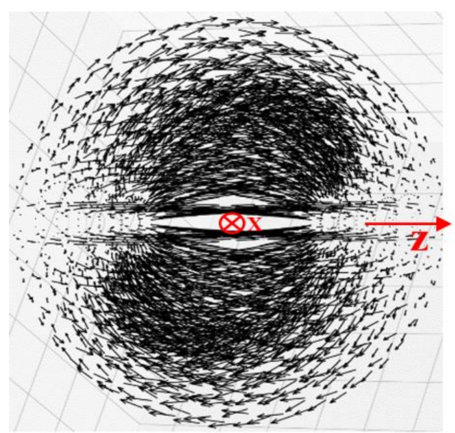

Fig. 5.1. The cross-section of the field of the velocity component $v_\phi^{(+b1)}$. of the a_1-subcont. Calculations were performed using the Mathlotlib library

The graphs of the functions $v_r^{(+a1)}(r)$ and $v_\phi^{(+a1)}(r)$ (45) depending on the distance r are shown in Figure 6.1.

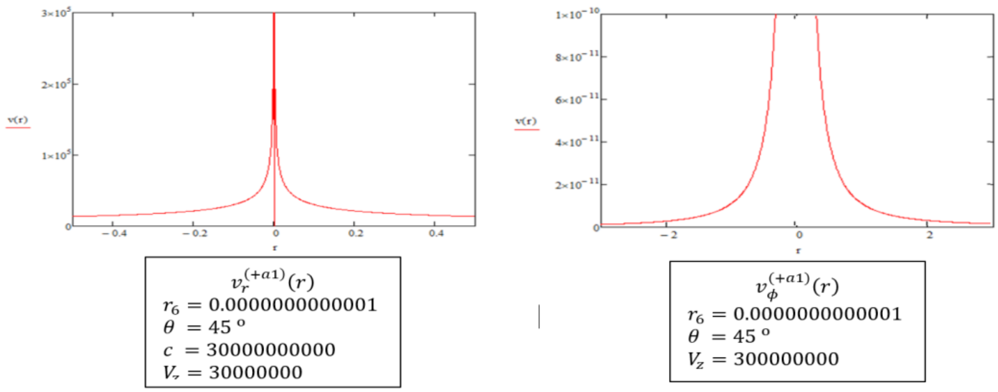

Fig. 6.1. Graphs of functions $v_r^{(+a1)}(r)$ and $v_\phi^{(+a1)}(r)$ (45)

Graphs of functions $v_r^{(+a1)}(\theta)$ and $v_\phi^{(+a1)}(\theta)$ (45) on angle θ for different values of r, V_z are shown in Figure 6.2.

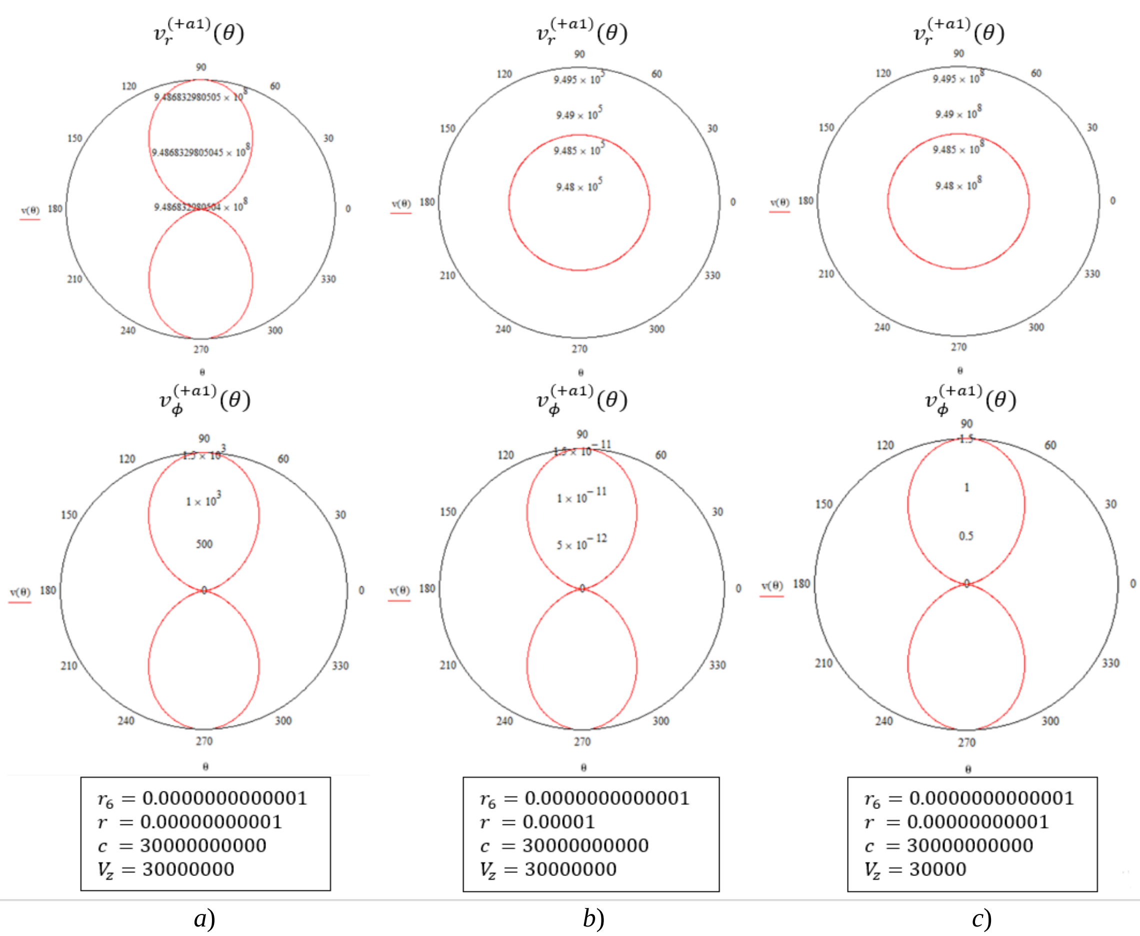

Fig. 6.2. Graphs of functions $v_r^{(+a1)}(\theta)$ and $v_\phi^{(+a1)}(\theta)$ (45) for different values of parameters r, V_z

By making similar comparisons of the components of the metric tensor from metrics (22) – (24) with the corresponding components from kinematic metrics (38) and (41), we obtain:

- components of the velocity vector $\vec{v}^{(+a1)}$ of the a_1-subcont

$$v_r^{(+a1)} \equiv c\sqrt{\frac{r_6 r}{r^2+a^2\cos^2\theta}}, \qquad v_\phi^{(+a1)} \equiv \frac{cr_6 a}{r^2+a^2\cos^2\theta}\sin^2\theta, \qquad v_\theta^{(+a1)} \equiv 0; \quad (46)$$

- components of the velocity vector $\vec{v}^{(+a2)}$ of the a_2-subcont

$$v_r^{(+a2)} \equiv c\sqrt{\frac{r_6 r}{r^2+a^2\cos^2\theta}}, \qquad v_\phi^{(+a2)} \equiv -\frac{cr_6 a}{r^2+a^2\cos^2\theta}\sin^2\theta, \qquad v_\theta^{(+a2)} \equiv 0; \quad (47)$$

- components of the velocity vector $\vec{v}^{(+b1)}$ of the b_1-subcont

$$v_r^{(+b1)} \equiv ic\sqrt{\frac{r_6 r}{r^2+a^2\cos^2\theta}}, \qquad v_\phi^{(+b1)} \equiv \frac{cr_6 a}{r^2+a^2\cos^2\theta}\sin^2\theta, \qquad v_\theta^{(+b1)} \equiv 0; \quad (48)$$

- components of the velocity vector $\vec{v}^{(+b2)}$ of the b_2-subcon

$$v_r^{(+b2)} \equiv ic\sqrt{\frac{r_6 r}{r^2+a^2\cos^2\theta}}, \qquad v_\phi^{(+b2)} \equiv -\frac{cr_6 a}{r^2+a^2\cos^2\theta}\sin^2\theta, \qquad v_\theta^{(+b2)} \equiv 0. \quad (49)$$

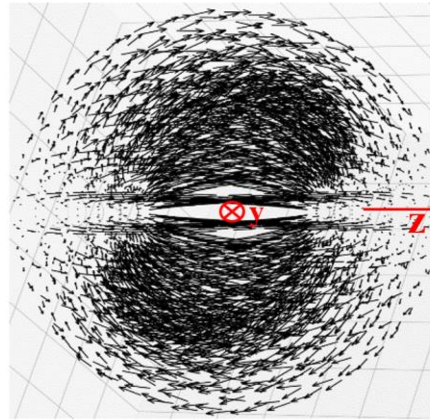

Fig. 5.2. The cross-section of the field of the velocity component $v_\phi^{(+b1)}$ of the b_1-subcontact is rotated by 90° around the Z axis

According to [4], for example,

$$v_\phi^{(+a,b1)} = v_\phi^{(+a1)} + iv_\phi^{(+b1)}, \qquad \left|v_\phi^{(+a,b1)}\right| = \sqrt{v_\phi^{(+a1)2} + v_\phi^{(+b1)2}}$$

This means that the components of the velocity vectors $v_\phi^{(+a1)}$ and $v_\phi^{(+b1)}$ are mutually perpendicular. Therefore, the field of the velocity component of the b_1-subcontact $v_\phi^{(+b1)}$ (see Figure 5.2) is perpendicular (i.e. rotated by 90° around the Z axis) with respect to the field of the velocity component of the a_1-subcontact $v_\phi^{(+a1)}$ (Figure 5.1).

An analysis of all four vector fields $\vec{v}^{(+a1)}$ (46), $\vec{v}^{(+a2)}$ (47), $\vec{v}^{(+b1)}$ (48), $\vec{v}^{(+b2)}$ (49) based on [4] shows that in the outer shell of the moving "electron" in the vicinity of its core, four toroidal-helical vortices are induced, which on average are reduced to two counter vortices (see Figure 7*a*,*b*). These counter toroidal-helical vortices compensate each other's manifestations, and therefore are not observed (see Figure 7*c*). In addition, in the outer shell of the moving "electron", subcont currents remain flowing away from its core and flowing toward this core (see §2.2 in [7]), which also on average compensate each other's manifestations.

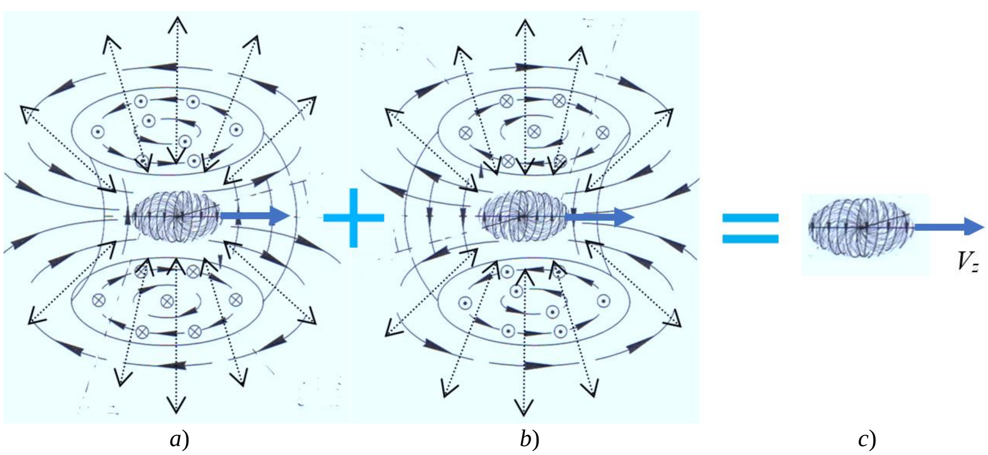

Fig. 7. In the outer shell (more precisely in the vicinity of the core) of an "electron" moving at a constant speed V_z on average, two counter toroidal-helical subcont vortices and two counter (inflowing and outflowing) subcont laminar currents are induced, which compensate for each other's manifestations

The model of an electron in the form of a spiral toroid was considered in the following works [13 – 21].

4.2 Estimation of the velocity of the antisubcont in the outer shell of the moving "positron"

Let's compare the zero components of the metric tensor from metrics (27) – (30) with the corresponding components from kinematic metrics (38) and (41), but with opposite signatures (– + + +)

$$ds^{(-)2} = -\left(1-\frac{v_r^2}{c^2}\right)c^2dt^2 - 2v_r dr dt + dr^2 + r^2d\theta^2 + r^2 sin^2\theta\, d\phi^2, \quad (50)$$

$$ds^{(-)2} = -\left(1-\frac{r^2\Omega^2}{c^2}\right)c^2dt^2 + dr^2 + r^2d\varphi^2 + dz^2 - \frac{2r^2\Omega^2}{c}d\varphi c dt. \quad (51)$$

As a result, we obtain:

- components of the velocity vector $\vec{v}^{(-a1)}$ of the a_1-antisubcont

$$v_r^{(-a1)} \equiv c\sqrt{\frac{r_6 r}{r^2+a^2\cos^2\theta}}, \quad v_\phi^{(-a1)} \equiv -\frac{cr_6a}{r^2+a^2\cos^2\theta}sin^2\theta, \quad v_\theta^{(-a1)} \equiv 0; \quad (52)$$

- components of the velocity vector $\vec{v}^{(-a2)}$ of the a_2-antisubcont

$$v_r^{(-a2)} \equiv c\sqrt{\frac{r_6 r}{r^2+a^2\cos^2\theta}}, \quad v_\phi^{(-a2)} \equiv \frac{cr_6a}{r^2+a^2\cos^2\theta}sin^2\theta, \quad v_\theta^{(-a2)} \equiv 0; \quad (53)$$

- components of the velocity vector $\vec{v}^{(-b1)}$ of the b_1-antisubcont

$$v_r^{(-b1)} \equiv ic\sqrt{\frac{r_6 r}{r^2+a^2\cos^2\theta}}, \quad v_\phi^{(-b1)} \equiv -\frac{cr_6a}{r^2+a^2\cos^2\theta}sin^2\theta, \quad v_\theta^{(-b1)} \equiv 0; \quad (54)$$

- components of the velocity vector $\vec{v}^{(-b2)}$ of the b_2-antisubcont

$$v_r^{(-b2)} \equiv ic\sqrt{\frac{r_6 r}{r^2+a^2\cos^2\theta}}, \quad v_\phi^{(-b2)} \equiv \frac{cr_6a}{r^2+a^2\cos^2\theta}sin^2\theta, \quad v_\theta^{(-b2)} \equiv 0. \quad (55)$$

A similar analysis of the four vector fields $\vec{v}^{(-a1)}$ (52), $\vec{v}^{(-a2)}$ (53), $\vec{v}^{(-b1)}$ (54), $\vec{v}^{(-b2)}$ (55) shows that in the outer shell of the moving "positron" in the vicinity of its core, four toroidal-helical vortices are induced, which on average are reduced to two counter vortices (see Figure 8*a*,*b*). These counter toroidal-helical vortices compensate each other's manifestations, and therefore are not observed (see Figure 8*c*). In addition, in the outer shell of the moving "positron" there are antisubcont currents flowing from its core and flowing to this core (see §2.2 in [7]), which also on average compensate each other's manifestations.

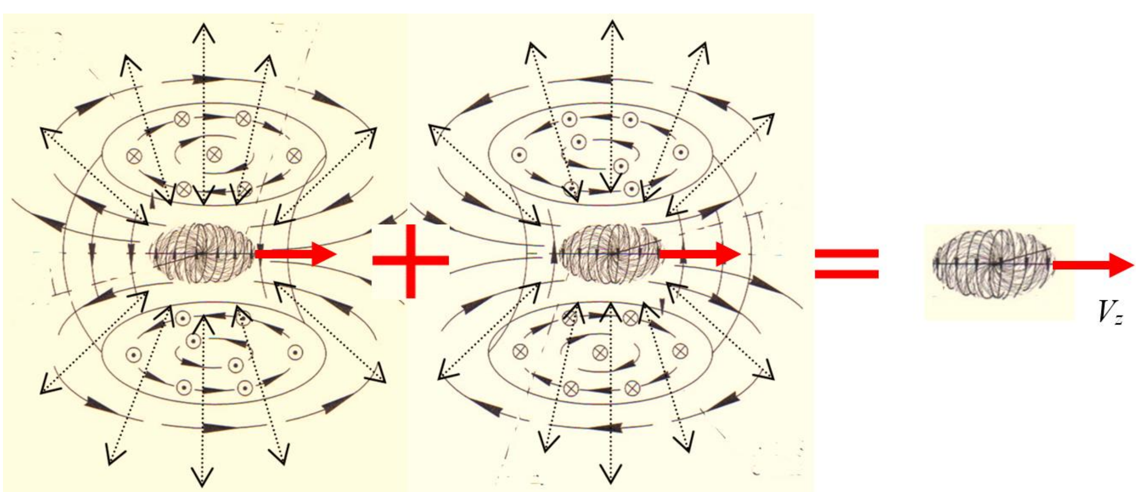

a) *b*) *c*)

Fig. 8. In the outer shell (more precisely in the vicinity of the core) of a "positron" moving at a constant speed *Vz*, on average, two counter toroidal-helical antisubcont vortices and two counter (inflowing and outflowing) antisubcont laminar currents are induced, which compensate for each other's manifestations

"Electron" and "positron", moving with the same speed V_z, in the same direction, are identical to each other. Only in the moving "positron" (i.e. in the conditional stable concavity of the $\lambda_{-12,-15}$-vacuum) all processes proceed in the opposite direction to the processes that proceed in the moving "electron" (i.e. in the conditional stable convexity of the $\lambda_{-12,-15}$-vacuum).

5 Acceleration of the subcont in the outer shell of a moving "electron"

5.1 Contravariant components of the metric tensor

We write out the expanded form of the Kerr metric (21), which describes the averaged behavior of the a1-subcont in the outer shell of a moving "electron"

$$s_1^{(+a1)2} = \left(1 - \frac{r_6 r}{r^2+a^2 cos^2\theta}\right) c^2 dt^2 - \frac{r^2+a^2 cos^2\theta}{r^2+a^2-rr_6} dr^2 - (r^2 + a^2 cos^2\theta) d\theta^2 - \left(r^2 + a^2 + \frac{r_6 r a^2 \sin^2\theta}{r^2+a^2 cos^2\theta}\right) sin^2\theta\, d\phi^2 + $$
$$+ \frac{2r_6 ra}{r^2+a^2cos^2\theta} sin^2\theta\, d\phi c dt. \tag{56}$$

The contravariant components of the metric tensor g^{ij} are equal to [8]

$$g^{ij} = \frac{\Delta_{ij}}{g}, \tag{57}$$

where is the algebraic complement of the corresponding element of the matrix (g_{ij}),

$$g = \|g_{ij}\| = -(r^2 + a^2 \cos^2\theta)^2 \sin^2\theta \text{ is the determinant of the matrix } (g_{ij}). \tag{58}$$

Calculations using Ex. (57) and the components of the metric tensor g_{ij} from the metric (56) resulted in the following components of the contravariant metric tensor [8]

$$g^{ij(+a1)} = \begin{pmatrix} \frac{(r^2+a^2)(r^2+a^2\cos^2\theta)+r_6 r a^2 \sin^2\theta}{(r^2+a^2-rr_6)(r^2+a^2\cos^2\theta)} & 0 & 0 & \frac{r_6 ra}{(r^2+a^2-rr_6)(r^2+a^2\cos^2\theta)} \\ 0 & -\frac{(r^2+a^2-rr_6)}{r^2+a^2\cos^2\theta} & 0 & 0 \\ 0 & 0 & -\frac{1}{r^2+a^2\cos^2\theta} & 0 \\ \frac{r_6 ra}{(r^2+a^2-rr_6)(r^2+a^2\cos^2\theta)} & 0 & 0 & -\frac{(r^2+a^2\cos^2\theta - rr_6)}{(r^2+a^2-rr_6)(r^2+a^2\cos^2\theta)\sin^2\theta} \end{pmatrix}. \tag{59}$$

5.2 Geometrized vectors of the a_1-subcont electric field strength and magnetic induction

The acceleration vector of the a1-subcont for the stationary case, which is the outer shell of the "electron" moving uniformly and rectilinearly, is determined by expressions of the form (95) in [4]

$$\vec{a}^{(+a1)} = \frac{c^2}{\sqrt{1-\frac{v_r^{(+a1)2}}{c^2}}} \left\{ -grad(ln\sqrt{g_{00}^{(+a1)}}) + \sqrt{g_{00}^{(+a1)}} \left[\frac{\vec{v}^{(+a1)}}{c} \times rot\vec{g}^{(+a1)}\right] \right\}, \tag{60}$$

where $\vec{g}^{(+a1)}(g_1^{(+a1)}, g_2^{(+a1)}, g_3^{(+a1)})$ is 3-dimensional vector with components $g_\alpha^{(+a1)} = -\frac{g_{0\alpha}^{(+a1)}}{g_{00}^{(+a1)}}$, (61)

or in component form (95) in [4]

$$a_\alpha^{(+a1)} = \frac{c^2}{\sqrt{1-\frac{v_r^{(+a1)2}}{c^2}}} \left\{ -\frac{\partial\, ln\sqrt{g_{00}^{(+a1)}}}{\partial x^\alpha} + \sqrt{g_{00}^{(+a1)}} \left(\frac{\partial g_\beta^{(+a1)}}{\partial x^\alpha} - \frac{\partial g_\alpha^{(+a1)}}{\partial x^\beta}\right) \frac{v_\beta^{(+a1)}}{c} \right\}, \tag{62}$$

where $v_\beta^{(+a1)}$ are the components of the 3-dimensional velocity vector $\vec{v}^{(+a1)}$ of the local section of the a_1-subcont, for the considered case of a moving "electron" according to (45)

$$v_r^{(+a1)} = c\sqrt{\frac{r_6 r}{r^2+a^2\cos^2\theta}}, \quad v_\phi^{(+a1)} = \frac{c r_6 a}{r^2+a^2 \cos^2\theta}\sin^2\theta, \quad v_\theta^{(+a1)} = 0. \tag{63}$$

According to Ex. (39)

$$v_r^{(+a1)2} = \frac{c^2 r_6 r}{r^2+a^2\cos^2\theta}. \tag{64}$$

In §5 in [4] it was shown that Ex. (60) can be represented in the following form (see Ex. (114) in [4])

$$\mathbf{a}^{(+a1)} = \mathbf{E}_o^{(+a1)} + [\mathbf{v}^{(+a1)} \times \mathbf{B}_o^{(+a1)}], \tag{65}$$

where $\mathbf{a}_E^{(+a1)} = \mathbf{E}_o^{(+a1}$ is the vector of the laminar (rectilinear) component of the acceleration of the a_1-subcontact ($\mathbf{a}_E^{(+a1)}$), its other name (in connection with the established tradition) is the geometrized vector of the a_1-subcont electrical intensity ($\mathbf{E}_o^{(+a1)}$) with components

$$a_{Er}^{(+a1)} = E_{or}^{(+a1)} = -\gamma\frac{\partial \ln\sqrt{g_{00}^{(+a1)}}}{\partial r_*}, \tag{66}$$
$$a_{E\theta}^{(+a1)} = E_{o\theta}^{(+a1)} = -\gamma\frac{\partial \ln\sqrt{g_{00}^{(+a1)}}}{\partial \theta_*},$$
$$a_{E\phi}^{(+a1)} = E_{o\phi}^{(+a1)} = -\gamma\frac{\partial \ln\sqrt{g_{00}^{(+a1)}}}{\partial \phi_*},$$

where $\gamma = \frac{c^2}{\sqrt{1-\frac{v_r^{(+a)2}}{c^2}}}$, (67)

$$\frac{\partial}{\partial r_*} = g^{11(+a1)}\frac{\partial}{\partial r}, \quad \frac{\partial}{\partial \theta_*} = g^{22(+a1)}\frac{\partial}{\partial \theta}, \quad \frac{\partial}{\partial \phi_*} = g^{33(+a1)}\frac{\partial}{\partial \phi}, \tag{68}$$

since the gradient of the scalar function $grad\, G(x,y,z) = \frac{\partial G}{dx}i + \frac{\partial G}{dy}j + \frac{\partial G}{dz}k$ in curved coordinates of the Riemannian space has the form [9] $\nabla G = e_i g^{ji}\frac{\partial G}{dx^j}$.

In turn, the curl of the vector **F**

$$rot\vec{F} = \left(\frac{\partial F_z}{\partial y} - \frac{\partial F_y}{\partial z}\right)i + \left(\frac{\partial F_x}{\partial z} - \frac{\partial F_z}{\partial x}\right)j + \left(\frac{\partial F_y}{\partial x} - \frac{\partial F_x}{\partial y}\right)k$$

in curved coordinates of Riemannian spaces has the form [9]

$$\frac{1}{\sqrt{|g|}}\frac{DF_j}{\partial x^i}e^{ijk} = \frac{1}{2\sqrt{|g|}}\left(\frac{\partial F_j}{\partial x^i} - \frac{\partial F_i}{\partial x^j}\right)e^{ijk},$$

where e^{ijk} is the Levi-Civita symbol.

Therefore, the turbulent (rotational) acceleration of the a_1-subcont [$\mathrm{v}^{(+a1)} \times \mathbf{B}_o^{(+a1)}$] from Ex. (65) in the component representation has the form:

$$a_{Br}^{(+a1)} = \left(v_\theta^{(+a1)} B_{0\phi}^{(+a1)} - v_\phi^{(+a1)} B_{0\theta}^{(+a1)}\right) = \frac{\gamma\sqrt{g_{00}^{(+a1)}}}{c}\left\{v_\theta^{(+a1)}\left(\frac{\partial g_\theta^{(+a1)}}{\partial r^+} - \frac{\partial g_r^{(+a1)}}{\partial \theta^+}\right) - v_\phi^{(+a1)}\left(\frac{\partial g_r^{(+a1)}}{\partial \phi^+} - \frac{\partial g_\phi^{(+a1)}}{\partial r^+}\right)\right\}, \qquad (69)$$

$$a_{B\theta}^{(+a1)} = \left(v_\phi^{(+a1)} B_{0r}^{(+a1)} - v_r^{(+a1)} B_{0\phi}^{(+a1)}\right) = \frac{\gamma\sqrt{g_{00}^{(+a1)}}}{c}\left\{v_\phi^{(+a1)}\left(\frac{\partial g_\phi^{(+a1)}}{\partial \theta^+} - \frac{\partial g_\theta^{(+a1)}}{\partial \phi^+}\right) - v_r^{(+a1)}\left(\frac{\partial g_\theta^{(+a1)}}{\partial r^+} - \frac{\partial g_r^{(+a1)}}{\partial \theta^+}\right)\right\},$$

$$a_{B\phi}^{(+a1)} = \left(v_r^{(+a1)} B_{0\theta}^{(+a1)} - v_\theta^{(+a1)} B_{0r}^{(+a1)}\right) = \frac{\gamma\sqrt{g_{00}^{(+a1)}}}{c}\left\{v_r^{(+a1)}\left(\frac{\partial g_r^{(+a1)}}{\partial \phi^+} - \frac{\partial g_\phi^{(+a1)}}{\partial r^+}\right) - v_\theta^{(+a1)}\left(\frac{\partial g_\phi^{(+a1)}}{\partial \theta^+} - \frac{\partial g_\theta^{(+a1)}}{\partial \phi^+}\right)\right\},$$

where $\frac{\partial}{\partial r^+} = \frac{1}{2\sqrt{|g|}}\frac{\partial}{\partial r}$, $\qquad \frac{\partial}{\partial \theta^+} = \frac{1}{2\sqrt{|g|}}\frac{\partial}{\partial \theta}$, $\qquad \frac{\partial}{\partial \phi^+} = \frac{1}{2\sqrt{|g|}}\frac{\partial}{\partial \phi}$.

Here $\mathbf{B}_o^{(+a1)}$ is the geometrized vector of a1-subcontact magnetic induction with components

$$B_{or}^{(-a)} = \frac{\gamma\sqrt{g_{00}^{(+a1)}}}{c}\left(\frac{\partial g_\phi^{(+a1)}}{\partial \theta^+} - \frac{\partial g_\theta^{(+a1)}}{\partial \phi^+}\right),\ B_{o\theta}^{(-a)} = \frac{\gamma\sqrt{g_{00}^{(+a1)}}}{c}\left(\frac{\partial g_r^{(+a1)}}{\partial \phi^+} - \frac{\partial g_\phi^{(+a1)}}{\partial r^+}\right),\ B_{o\phi}^{(-a)} = \frac{\gamma\sqrt{g_{00}^{(+a1)}}}{c}\left(\frac{\partial g_\theta^{(+a1)}}{\partial r^+} - \frac{\partial g_r^{(+a1)}}{\partial \theta^+}\right). \quad (70)$$

The geometrized Ex. (65) is similar to the Lorentz force in classical electrodynamics. However, within the framework of Geometrized vacuum physics (GVPh), the cause of electromagnetism is not some phenomenological electromagnetic field, but accelerated laminar and turbulent flows (currents), in particular, the a_1-subcontact, which are described by geometrized vectors $\mathbf{E}_o^{(+a1)}$ and $\mathbf{B}_o^{(+a1)}$ with components

$$(71)$$

$$E_{or}^{(+a1)} = -\gamma\frac{\partial\, ln\sqrt{g_{00}^{(+a1)}}}{\partial r_*}, \qquad B_{or}^{(+a1)} = \frac{\gamma\sqrt{g_{00}^{(+a1)}}}{c}\left(\frac{\partial g_\phi^{(+a1)}}{\partial \theta^+} - \frac{\partial g_\theta^{(+a1)}}{\partial \phi^+}\right),$$

$$E_{o\theta}^{(+a1)} = -\gamma\frac{\partial\, ln\sqrt{g_{00}^{(+a1)}}}{\partial \theta_*}, \qquad B_{o\theta}^{(+a1)} = \frac{\gamma\sqrt{g_{00}^{(+a1)}}}{c}\left(\frac{\partial g_r^{(+a1)}}{\partial \phi^+} - \frac{\partial g_\phi^{(+a1)}}{\partial r^+}\right),$$

$$E_{o\phi}^{(+a1)} = -\gamma\frac{\partial\, ln\sqrt{g_{00}^{(+a1)}}}{\partial \phi_*}; \qquad B_{o\phi}^{(+a1)} = \frac{\gamma\sqrt{g_{00}^{(+a1)}}}{c}\left(\frac{\partial g_\theta^{(+a1)}}{\partial r^+} - \frac{\partial g_r^{(+a1)}}{\partial \theta^+}\right).$$

5.2 Acceleration of the a1-subcontact in the outer shell of a moving "electron"

We write out the zero components of the metric tensor from the metric (56)

$$g_{00}^{(+a1)} = 1 - \frac{r_6 r}{r^2 + a^2\cos^2\theta}, \qquad g_{01}^{(+a1)} = g_{02}^{(+a1)} = 0, \qquad g_{03}^{(+a1)} = \frac{2r_6 ra\sin^2\theta}{r^2 + a^2\cos^2\theta}. \qquad (72)$$

. .

In this case, according to Ex. (61) $g_\alpha^{(+a1)} = -\frac{g_{0\alpha}^{(+a1)}}{g_{00}^{(+a1)}}$, we have

$$g_r^{(+a1)} = -\frac{g_{01}^{(+a1)}}{g_{00}^{(+a1)}} = 0, \qquad g_\theta^{(+a1)} = -\frac{g_{02}^{(+a1)}}{g_{00}^{(+a1)}} = 0, \qquad g_\phi^{(+a1)} = -\frac{g_{03}^{(+a1)}}{g_{00}^{(+a1)}} = -\frac{2r_6 ra\sin^2\theta}{r^2 + a^2\cos^2\theta - r_6 r}, \qquad (73)$$

also for the case under consideration, according to Exs. (64) and (67)

$$\gamma = \frac{c^2}{\sqrt{1-\frac{v_r^{(+a1)2}}{c^2}}} = \frac{c^2}{\sqrt{1-\frac{r_6 r}{\rho}}} = \frac{c^2}{\sqrt{g_{00}^{(+\alpha1)}}} \,. \tag{74}$$

Let's write out the contravariant components (59) of the metric (56)

$$g^{11(+a1)} = -\frac{(r^2+a^2-rr_6)}{r^2+a^2\cos^2\theta}, \quad g^{22(+a1)} = -\frac{1}{r^2+a^2\cos^2\theta}, \quad g^{33(+a1)} = -\frac{(r^2+a^2\cos^2\theta-rr_6)}{(r^2+a^2-rr_6)(r^2+a^2\cos^2\theta)\sin^2\theta}\,. \tag{75}$$

We find the components of the vector of the geometrized subcont electrical intensity $\mathbf{E}_o^{(+\alpha1)}$ (i.e. the components of the acceleration vector that determines the laminar component of the acceleration of the a_1-subcontact) (66). Taking into account Exs. (72) – (75), we obtain

$$a_{Er}^{(+a1)} = E_{or}^{(+a1)} = -\frac{c^2}{\sqrt{g_{00}^{(+\alpha1)}}} g^{11(+a1)} \frac{\partial \ln\sqrt{g_{00}{}^{(+a1)}}}{\partial r} = -\frac{c^2 r_6(r^2+a^2-rr_6)(r^2-a^2\cos^2)}{2\left(1-\frac{r_6 r}{r^2+a^2\cos^2\theta}\right)^{\frac{3}{2}}(r^2+a^2\cos^2\theta)^3}\,, \tag{76}$$

$$a_{E\theta}^{(+a1)} = E_{o\theta}^{(+a1)} = -\frac{c^2}{\sqrt{g_{00}^{(+\alpha1)}}} g^{22(+a1)} \frac{\partial \ln\sqrt{g_{00}^{(+a1)}}}{\partial\theta} = \frac{c^2 r r_6 a^2 \sin 2\theta}{2\left(1-\frac{r_6 r}{r^2+a^2\cos^2\theta}\right)^{\frac{3}{2}}(r^2+a^2\cos^2\theta)^3}\,, \tag{77}$$

$$a_{E\phi}^{(+a1)} = E_{o\phi}^{(+a1)} = -\frac{c^2}{\sqrt{g_{00}^{(+\alpha1)}}} g^{33(+a1)} \frac{\partial \ln\sqrt{g_{00}^{(+a1)}}}{\partial\phi} = 0. \tag{78}$$

где согласно (25′) $a = \frac{r_6 V_z}{2c}$ – параметр эллиптичности.

Attention! *The dimension of the component $E_{o\theta}^{(+a1)}$ (77) 1/sec² differs from the dimension of acceleration m/sec² of the component $E_{o\theta}^{(+a1)}$ (76). The dimension 1/sec² corresponds to the dimension of acceleration of the angular velocity of rotation dΩ/dt. The angular velocity is related to the linear velocity by the relation v = rΩ, Differentiate this relation with respect to time, then dv/dt= rdΩ/dt. Therefore, we multiply Ex. (77) by r*

$$a_{E\theta}^{(+a1)} = rE_{o\theta}^{(+a1)} = -\frac{rc^2}{\sqrt{g_{00}^{(+\alpha1)}}} g^{22(+a1)} \frac{\partial \ln\sqrt{g_{00}^{(+a1)}}}{\partial\theta} = \frac{c^2 r^2 r_6 a^2 \sin 2\theta}{2\left(1-\frac{r_6 r}{r^2+a^2\cos^2\theta}\right)^{\frac{3}{2}}(r^2+a^2\cos^2\theta)^3}\,. \tag{77′}$$

This situation requires rechecking and additional understanding.

At a = 0, the components of the vector of the geometrized electrical intensity of the a_1-subcont $E_{or}^{(+a1)} = a_{Er}^{(+a1)}$ (76) – (78) are reduced to the form of Exs. (55) in [7]

$$E_{vr}^{(+a1)} = a_{Er}^{(+a1)} = -\frac{c^2 r_6}{2r^2\sqrt{\left(1-\frac{r_6}{r}\right)}}, \quad E_\theta^{(+a1)} = 0, \quad E_\phi^{(+a1)} = 0, \quad \text{with the dimension } m/sec^2. \tag{79}$$

This confirms the correctness of the obtained results.

The graphs of functions (76) and (77′) for the conventionally accepted values: $c = 1$, $r_6 = 10^{-14}$, $r = 10^{-13}$ and V_z = 0,00001 are shown in Figure 9.

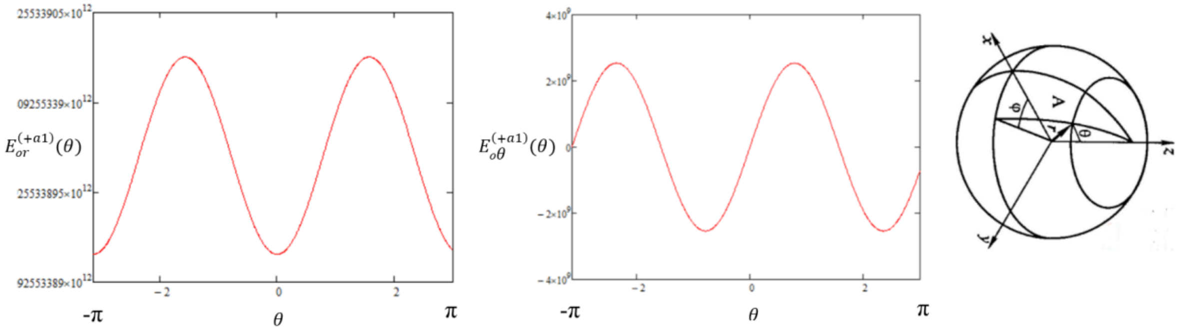

Fig. 9. Graphs of functions (76) and (77′) for the conventionally accepted values:
$c = 1,\ r_6 = 10^{-14},\ r = 10^{-13}$, and $V_z = 0{,}00001$

When substituting Exs. (58), (72) – (75) into (70) for the components of the vector a_1-subcont geometrized magnetic induction $\mathbf{B}_o^{(+\alpha 1)}$ in the outer shell of a free valence "electron" moving rectilinearly at a constant velocity, we obtain:

$$B_{or}^{(+\alpha1)} = \frac{\gamma\sqrt{g_{00}^{(+\alpha1)}}}{2c\sqrt{|g|}}\left(\frac{\partial g_{\phi}^{(+\alpha1)}}{\partial\theta} - \frac{\partial g_{\theta}^{(+\alpha1)}}{\partial\phi}\right) = -\frac{2crr_6 a\cos\theta(r^2+a^2-r_6 r)}{(r^2+a^2\cos^2\theta)(r^2+a^2\cos^2\theta-r_6 r)^2}, \qquad (80)$$

$$B_{o\theta}^{(+\alpha1)} = \frac{\gamma\sqrt{g_{00}^{(+\alpha1)}}}{2c\sqrt{|g|}}\left(\frac{\partial g_{r}^{(+\alpha1)}}{\partial\phi} - \frac{\partial g_{\phi}^{(+\alpha1)}}{\partial r}\right) = \frac{cr_6 a\sin\theta(a^2\cos^2\theta-r^2)}{(r^2+a^2\cos^2\theta)(r^2+a^2\cos^2\theta-r_6 r)^2}, \qquad (81)$$

$$B_{o\phi}^{(+\alpha1)} = \frac{\gamma\sqrt{g_{00}^{(+\alpha1)}}}{2c\sqrt{|g|}}\left(\frac{\partial g_{\theta}^{(+\alpha1)}}{\partial r} - \frac{\partial g_{r}^{(+\alpha1)}}{\partial\theta}\right) = 0. \qquad (82)$$

Attention! *The dimension of the component $B_{or}^{(+\alpha1)}$ (80) is 1/sec (corresponds to the dimension of the angular velocity of rotation), and the dimension of the component $B_{o\theta}^{(+\alpha1)}$ (82) is 1/(sec·m).*

Substituting the components of the subcont induction vector $\mathbf{B}_o^{(+\alpha1)}$ (80) – (82) and the velocity (63) into the expressions for the components of the turbulent (rotational) acceleration a_1-subcont of the form (69) for the outer shell of a free "electron" moving with a constant velocity V_z , we obtain:

$$a_{Br}^{(+\alpha1)} = \left(-v_{\phi}^{(+\alpha1)}B_{o\theta}^{(+\alpha1)}\right) = -\frac{v_{\phi}^{(+\alpha1)}cr_6 a\sin\theta(a^2\cos^2\theta-r^2)}{(r^2+a^2\cos^2\theta)(r^2+a^2\cos^2\theta-r_6 r)^2} = -\sqrt{\frac{r_6 r}{r^2+a^2\cos^2\theta}}\,\frac{c^2 r_6 a\sin\theta(a^2\cos^2\theta-r^2)}{(r^2+a^2\cos^2\theta)(r^2+a^2\cos^2\theta-r_6 r)^2}, \qquad (83)$$

$$a_{B\theta}^{(+\alpha1)} = \left(v_{\phi}^{(+\alpha1)}B_{or}^{(+\alpha1)}\right) = -\frac{v_{\phi}^{(+\alpha1)}2cr_6 a\cos\theta(r^2+a^2-r_6 r)}{(r^2+a^2\cos^2\theta)(r^2+a^2\cos^2\theta-r_6 r)^2} = -\frac{2c^2 r_6^2 a^2\cos\theta\sin^2\theta(r^2+a^2-r_6 r)}{(r^2+a^2\cos^2\theta)^2(r^2+a^2\cos^2\theta-r_6 r)^2}, \qquad (84)$$

$$a_{B\phi}^{(+\alpha1)} = \left(v_{r}^{(+\alpha1)}B_{o\theta}^{(+\alpha1)}\right) = \frac{v_{r}^{(+\alpha1)}cr_6 a\sin\theta(a^2\cos^2\theta-r^2)}{(r^2+a^2\cos^2\theta)(r^2+a^2\cos^2\theta-r_6 r)^2} = \sqrt{\frac{r_6 r}{r^2+a^2\cos^2\theta}}\,\frac{c^2 r_6 a\sin\theta(a^2\cos^2\theta-r^2)}{(r^2+a^2\cos^2\theta)(r^2+a^2\cos^2\theta-r_6 r)^2}. \qquad (85)$$

We substitute the components of the laminar acceleration vector (76), (77′), (78) and the components of the turbulent acceleration vector (83) − (85) into equations (69), as a result we obtain the following components of the a_1-subcont acceleration vector $\mathbf{a}^{(+\alpha1)}$ in the outer shell of the "electron" moving with a constant velocity V_z in the direction of the Z axis

$$a_r^{(+a1)} = a_{Er}^{(+a1)} + a_{Br}^{(+a1)} = \frac{c^2 r_6 (r^2+a^2-rr_6)(r^2-a^2\cos^2\theta)}{2\left(1-\frac{r_6 r}{r^2+a^2\cos^2\theta}\right)^{\frac{3}{2}}(r^2+a^2\cos^2\theta)^3} - \sqrt{\frac{r_6 r}{r^2+a^2\cos^2\theta}}\frac{c^2 r_6 a \sin\theta(a^2\cos^2\theta-r^2)}{(r^2+a^2\cos^2\theta)(r^2+a^2\cos^2\theta-r_6 r)^2}, \quad (86)$$

$$a_\theta^{(+a1)} = a_{E\theta}^{(+a1)} + a_{B\theta}^{(+a1)} = \frac{c^2 r r_6 a^2 \sin 2\theta}{2\left(1-\frac{r_6 r}{r^2+a^2\cos^2\theta}\right)^{\frac{3}{2}}(r^2+a^2\cos^2\theta)^3} - \frac{2c^2 r_6^2 a^2 \cos\theta \sin^2\theta(r^2+a^2-r_6 r)}{(r^2+a^2\cos^2\theta)^2(r^2+a^2\cos^2\theta-r_6 r)^2}, \quad (87)$$

$$a_\phi^{(+a1)} = a_{E\phi}^{(+a1)} + a_{B\phi}^{(+a1)} = \sqrt{\frac{r_6 r}{r^2+a^2\cos^2\theta}}\frac{c^2 r_6 a \sin\theta(a^2\cos^2\theta-r^2)}{(r^2+a^2\cos^2\theta)(r^2+a^2\cos^2\theta-r_6 r)^2}, \quad (89)$$

where according to (25´) $a = \frac{r_6 V_z}{2c}$ is the ellipticity parameter.

The graph of functions (70), (71) and (72) with the conventionally accepted values: $c = 1$, $r_6 = 10^{-14}$, $r = 10^{-12}$ and $V_z = 0.0000001$ are shown in Figure 10.

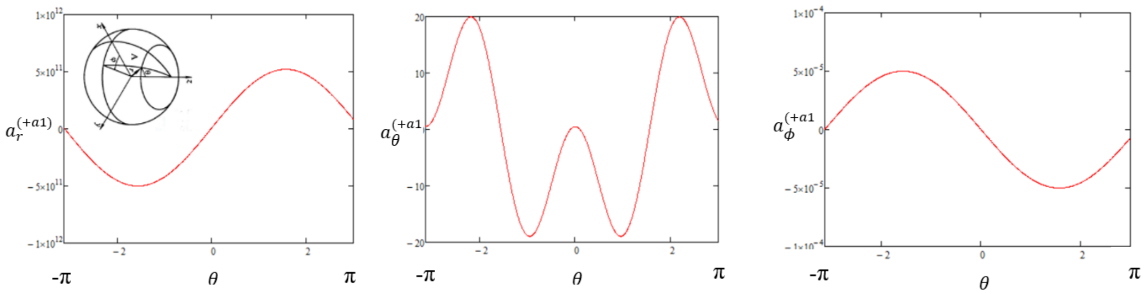

Fig. 10. Graphs of functions (70), (71) and (72) with the conventionally accepted: $c = 1$, $r_6 = 10^{-14}$, $r = 10^{-12}$ and $V_z = 0{,}0000001$

5.3 Acceleration of a_2-subcont, b_1-subcont and b_2-subcont in the outer shell of a moving "electron"

Performing actions similar to (56) – (89) with the metrics-solutions of the Einstein vacuum equation (22) – (24)

$$ds_2^{(+a2)2} = \left(1-\frac{r_6 r}{\rho}\right)c^2dt^2 - \frac{\rho dr^2}{\Delta^{(a)}} - \rho d\theta^2 - \left(r^2+a^2+\frac{r_6 r a^2}{\rho}\sin^2\theta\right)\sin^2\theta\, d\phi^2 - \frac{2r_6 r a}{\rho}\sin^2\theta\, d\phi c dt, \quad (22')$$

$$ds_3^{(+b1)2} = \left(1+\frac{r_6 r}{\rho}\right)c^2dt^2 - \frac{\rho dr^2}{\Delta^{(b)}} - \rho d\theta^2 - \left(r^2+a^2-\frac{r_6 r a^2}{\rho}\sin^2\theta\right)\sin^2\theta\, d\phi^2 + \frac{2r_6 r a}{\rho}\sin^2\theta\, d\phi c dt, \quad (23')$$

$$ds_4^{(+b1)2} = \left(1+\frac{r_6 r}{\rho}\right)c^2dt^2 - \frac{\rho dr^2}{\Delta^{(b)}} - \rho d\theta^2 - \left(r^2+a^2-\frac{r_6 r a^2}{\rho}\sin^2\theta\right)\sin^2\theta\, d\phi^2 - \frac{2r_6 r a}{\rho}\sin^2\theta\, d\phi c dt, \quad (24')$$

we obtain for the outer shell of the "electron" moving with a constant velocity V_z in the direction of the Z axis:

- components of the vector of a_2-subcont acceleration $\mathbf{a}^{(+a2)}$

$$a_r^{(+a2)} = a_{Er}^{(+a2)} + a_{Br}^{(+a2)} = \frac{c^2 r_6 (r^2+a^2-rr_6)(r^2-a^2\cos^2\theta)}{2\left(1-\frac{r_6 r}{r^2+a^2\cos^2\theta}\right)^{\frac{3}{2}}(r^2+a^2\cos^2\theta)^3} + \sqrt{\frac{r_6 r}{r^2+a^2\cos^2\theta}}\frac{c^2 r_6 a \sin\theta(a^2\cos^2\theta-r^2)}{(r^2+a^2\cos^2\theta)(r^2+a^2\cos^2\theta-r_6 r)^2}, \quad (90)$$

$$a_\theta^{(+a2)} = a_{E\theta}^{(+a2)} + a_{B\theta}^{(+a2)} = \frac{c^2 r r_6 a^2 \sin 2\theta}{2\left(1-\frac{r_6 r}{r^2+a^2\cos^2\theta}\right)^{\frac{3}{2}}(r^2+a^2\cos^2\theta)^3} + \frac{2c^2 r_6^2 a^2 \cos\theta \sin^2\theta(r^2+a^2-r_6 r)}{(r^2+a^2\cos^2\theta)^2(r^2+a^2\cos^2\theta-r_6 r)^2}, \quad (91)$$

$$a_\phi^{(+a1)} = a_{E\phi}^{(+a2)} + a_{B\phi}^{(+a2)} = -\sqrt{\frac{r_6 r}{r^2+a^2\cos^2\theta}}\frac{c^2 r_6 a \sin\theta(a^2\cos^2\theta-r^2)}{(r^2+a^2\cos^2\theta)(r^2+a^2\cos^2\theta-r_6 r)^2}; \quad (92)$$

- components of the vector of b_1-subcont acceleration $\mathbf{a}^{(+b1)}$

$$a_r^{(+a2)} = a_{Er}^{(+b1)} + a_{Br}^{(+b1)} = \frac{c^2 r_6 (r^2+a^2-rr_6)(r^2-a^2 \cos^2\theta)}{2\left(1+\frac{r_6 r}{r^2+a^2\cos^2\theta}\right)^{\frac{3}{2}}(r^2+a^2\cos^2\theta)^3} - \sqrt{\frac{r_6 r}{r^2+a^2\cos^2\theta}}\,\frac{c^2 r_6 a \sin\theta(a^2\cos^2\theta+r^2)}{(r^2+a^2\cos^2\theta)(r^2+a^2\cos^2\theta-r_6 r)^2}, \tag{93}$$

$$a_\theta^{(+b1)} = a_{E\theta}^{(+b1)} + a_{B\theta}^{(+b1)} = \frac{c^2 r r_6 a^2 \sin 2\theta}{2\left(1+\frac{r_6 r}{r^2+a^2\cos^2\theta}\right)^{\frac{3}{2}}(r^2+a^2\cos^2\theta)^3} - \frac{2c^2 r_6^2 a^2 \cos\theta \sin^2\theta(r^2+a^2-r_6 r)}{(r^2+a^2\cos^2\theta)^2(r^2+a^2\cos^2\theta-r_6 r)^2}, \tag{94}$$

$$a_\phi^{(+b1)} = a_{E\phi}^{(+b1)} + a_{B\phi}^{(+b1)} = \sqrt{\frac{r_6 r}{r^2+a^2\cos^2\theta}}\,\frac{c^2 r_6 a \sin\theta(a^2\cos^2\theta+r^2)}{(r^2+a^2\cos^2\theta)(r^2+a^2\cos^2\theta-r_6 r)^2}; \tag{95}$$

- components of the vector of b_2-subcont acceleration $\mathbf{a}^{(+b2)}$

$$a_r^{(+b2)} = a_{Er}^{(+b2)} + a_{Br}^{(+b2)} = \frac{c^2 r_6 (r^2+a^2-rr_6)(r^2-a^2 \cos^2\theta)}{2\left(1+\frac{r_6 r}{r^2+a^2\cos^2\theta}\right)^{\frac{3}{2}}(r^2+a^2\cos^2\theta)^3} + \sqrt{\frac{r_6 r}{r^2+a^2\cos^2\theta}}\,\frac{c^2 r_6 a \sin\theta(a^2\cos^2\theta+r^2)}{(r^2+a^2\cos^2\theta)(r^2+a^2\cos^2\theta-r_6 r)^2}, \tag{96}$$

$$a_\theta^{(+b2)} = a_{E\theta}^{(+b2)} + a_{B\theta}^{(+b2)} = \frac{c^2 r r_6 a^2 \sin 2\theta}{2\left(1+\frac{r_6 r}{r^2+a^2\cos^2\theta}\right)^{\frac{3}{2}}(r^2+a^2\cos^2\theta)^3} + \frac{2c^2 r_6^2 a^2 \cos\theta \sin^2\theta(r^2+a^2-r_6 r)}{(r^2+a^2\cos^2\theta)^2(r^2+a^2\cos^2\theta-r_6 r)^2}, \tag{97}$$

$$a_\phi^{(+b2)} = a_{E\phi}^{(+b2)} + a_{B\phi}^{(+b2)} = -\sqrt{\frac{r_6 r}{r^2+a^2\cos^2\theta}}\,\frac{c^2 r_6 a \sin\theta(a^2\cos^2\theta+r^2)}{(r^2+a^2\cos^2\theta)(r^2+a^2\cos^2\theta-r_6 r)^2}. \tag{98}$$

Attention! We urge mathematicians to double-check the obtained Exs. (86) – (98).

5.4 Accelerated vacuum currents in the outer shell of a moving "electron"

The general vector field of accelerated vacuum currents in the outer shell of a moving "electron", according to geometrized vacuum electrodynamics (see [4], especially §5 and 6 in [4]), is defined as a vector-quaternion

$$\mathbf{a}_\Sigma^{(+ab)} = \frac{1}{4}(\mathbf{a}^{(+a1)} + i\mathbf{a}^{(+a2)} + j\mathbf{a}^{(+b1)} + k\mathbf{a}^{(+b2)}), \tag{99}$$

where

$\mathbf{a}^{(+a1)} = \mathbf{E}_o^{(+a1)} + [\mathbf{v}^{(+a1)} \times \mathbf{B}_o^{(+a1)}]$ is vector field of accelerations of a_1-subcont (86) – (89); (100)

$\mathbf{a}^{(+a2)} = \mathbf{E}_o^{(+a2)} + [\mathbf{v}^{(+a2)} \times \mathbf{B}_o^{(+a2)}]$ is vector field of accelerations of a_2-subcont (90) – (92);

$\mathbf{a}^{(+b1)} = \mathbf{E}_o^{(+b1)} + [\mathbf{v}^{(+b1)} \times \mathbf{B}_o^{(+b1)}]$ is vector field of accelerations of b_1-subcont (93) – (95);

$\mathbf{a}^{(+b2)} = \mathbf{E}_o^{(+b2)} + [\mathbf{v}^{(+b2)} \times \mathbf{B}_o^{(+b2)}]$ is vector field of accelerations of b_2-subcont (96) – (98).

This type of notation for the general vector field of vacuum accelerations is due to the fact that the current lines of accelerated a_k-subcont and b_k-subcont currents are intertwined into current bundles.

Ex. (100) can be represented in expanded form

$$\mathbf{a}_\Sigma^{(+ab)} = \frac{1}{4}(\mathbf{E}_o^{(+a1)} + i\mathbf{E}_o^{(+a2)} + j\mathbf{E}_o^{(+b1)} + k\,\mathbf{E}_o^{(+b2)}) + \frac{1}{4}([\mathbf{v}^{(+a1)} \times \mathbf{B}_o^{(+a1)}] + i[\mathbf{v}^{(+a2)} \times \mathbf{B}_o^{(+a2)}] + j[\mathbf{v}^{(+b1)} \times \mathbf{B}_o^{(+b1)}] + k\,[\mathbf{v}^{(+b2)} \times \mathbf{B}_o^{(+b2)}]). \tag{101}$$

or $\mathbf{a}_\Sigma^{(+ab)} = \mathbf{E}_\Sigma^{(+ab)} + [\mathbf{v}_\Sigma^{(+ab)} \times \mathbf{B}_\Sigma^{(+ab)}]$, (102)

where, in the case of uniform and rectilinear motion of the "electron",

$$\mathbf{E}_{\Sigma}{}^{(+ab)} = \frac{1}{4}\,(\mathbf{E}_{o}{}^{(+a1)} + i\mathbf{E}_{o}{}^{(+a2)} + j\mathbf{E}_{o}{}^{(+b1)} + k\mathbf{E}_{o}{}^{(+b2)}) \qquad (103)$$

is the total geometrized field of the vector of the laminar (rectilinear) component of the subcont acceleration in the outer shell of the moving "electron", or the averaged geometrized vector of the subcont electrical field strength;

$$\mathbf{B}_{\Sigma}{}^{(+ab)} = \frac{1}{4}\,(\mathbf{B}_{o}{}^{(+a1)} + i\mathbf{B}_{o}{}^{(+a2)} + j\mathbf{B}_{o}{}^{(+b1)} + k\mathbf{B}_{o}{}^{(+b2)}) \qquad (104)$$

is the total geometrized field of the vector of the turbulent (rotational) component of the subcont acceleration in the outer shell of the moving "electron", or the averaged geometrized vector of the subcont magnetic induction;

$$\mathbf{v}_{\Sigma}{}^{(+ab)} = \frac{1}{4}\,(\mathbf{v}^{(+a1)} + i\mathbf{v}^{(+a2)} + j\mathbf{v}^{(+b1)} + k\mathbf{v}^{(+b2)}) \qquad (105)$$

is the total field of the subcont velocity vector in the outer shell of the moving "electron".

Vector quaternion (99) describes an extremely complex interweaving of subcont currents in the outer shell of an "electron" moving rectilinearly and uniformly with a constant velocity V_z. Recall that this article considers the simplest version of interweaving only a_k-subcon currents with the same topology, i.e. with one signature (+ – – –). However, it is necessary to remember that each a_k-subcont current can be represented as an interweaving of seven subcurrents with different signatures (see [2,3,4]). Therefore, at a deeper level of consideration, the picture of intra-vacuum processes in the outer shell of a free moving "electron" looks even more complex, but at the same time more elegant and harmonious. In Figure 11 an attempt is made to illustrate the interweaving of a_k-subcont currents and sub-currents, with the sub-currents labeled with one of the seven rainbow colors (red, orange, yellow, green, blue, indigo, violet), which correspond to the signature of their $\lambda_{-12,-15}$-vacuum sub-layer (see (123) in [5]).

Fig. 11. Illustration of the interweaving of $\lambda_{-12,-15}$-vacuum sub-currents, tied into knots and twisted into spirals.
This illusion is inspired by the mathematical apparatus of geometrized vacuum physics,
based on the Algebra of signatures (see [2,3,4,5,6,7])

We anticipate the objection that in the geometrized physics of vacuum there is no constructive concept of the substantiality of subcont currents, just as the substantiality of the electromagnetic field is unclear in classical electrodynamics. Within the framework of purely geometric constructions, the subcont (i.e., a complexly woven pseudo-medium) forms only the illusion of concepts of intra-vacuum processes. Nevertheless, the logical apparatus based on the geometrized vectors $\mathbf{E}_o^{(+\alpha k)}$ and $\mathbf{B}_o^{(+\alpha k)}$, associated respectively with the laminar and turbulent acceleration of one of the layers of the pseudo-medium (in particular, the a_1-subcont), is significantly more subtle and understandable, in comparison with the heuristic mathematical apparatus of classical electrodynamics, where the concepts of electric and magnetic fields are introduced directly on the basis of empirical phenomenology. Moreover, in our opinion, geometrized vacuum dynamics based on Signature Algebra meets the criteria of the Clifford-Einstein-Wheeler program, which is aimed at the complete geometrization of physics.

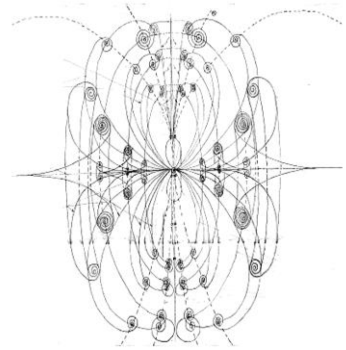

Fig. 12. Drawing by Lebedev V.A.

5.5 Simplified schematic representation of the outer shell of a moving "electron"

The vector-quaternion field of accelerations of four intertwined subcont layers in the outer shell of a moving "electron", described by Ex. (99), is extremely complex. However, upon averaging and at a significant distance from the core, the following simplified schematic representation of the vacuum region under study can be distinguished from this complex manifold.

The averaged field of the geometrized vector of subcont magnetic induction $\mathbf{B}_\Sigma^{(+ab)}$ describes a complex rotational-translational motion of the subcont layers around the direction of motion. This rotation is two counter toroidal-helical vortices, see Figure 7 (which are conventionally shown in Figure 13 as a single vortex, for ease of perception), induced around the core of the moving "electron" (Figure 13*b*).

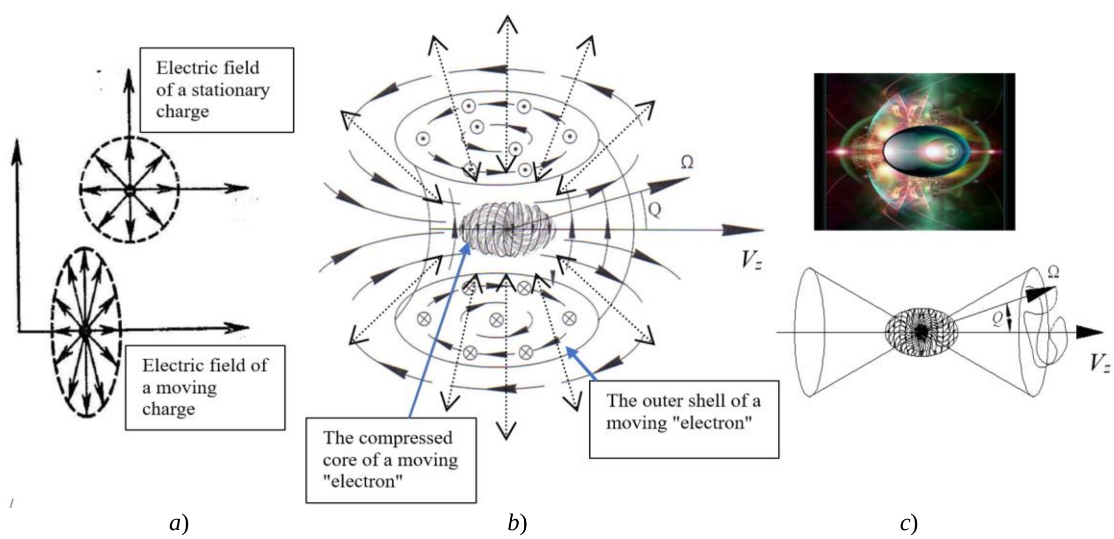

Fig. 13. *a*) The electric field of a charge at rest has spherical symmetry, and the electric field of a moving charge corresponds to the shape of an ellipsoid of revolution. *b*) Simplified diagram of accelerated laminar and turbulent subcont currents in the outer shell of an "electron" moving rectilinearly at a constant speed in the vacuum of which it itself consists. *c*) Precession of the axis of rotation of the core of a moving "electron" in a sector limited by a solid angle *Q*, around the direction *Z* of its uniform and rectilinear motion

The field of the averaged geometrized vector of the subcont electric intensity $\mathbf{E}_{\Sigma}^{(+ab)}$ in the outer shell of the moving "electron" is flattened (see Figure 13*a*,*b*). This field describes the accelerated laminar currents of various layers of the subcont, which flow in and out along spirals from/to the surface of the "electron" (see § 2.2.2 in [7]). But in this case, the field of the subcont electric intensity is not spherical in nature, as in the case of a stationary "electron" (see Figures 9 and 11 in [7]), but has the character of an ellipsoid of revolution, flattened along the Z axis, which coincides with the direction of motion of the "electron".

These ideas of Geometrized vacuum physics (GVPh) about a moving "electron" largely coincide with the conclusions of classical electrodynamics, according to which the electric field of a moving electron is flattened (as a result of relativistic effects), and a magnetic field is induced around it [10].

From the point of view of an outside observer, the core of a moving "electron" takes the form of an elongated ellipsoid (see Figure 13*b*,*c*), and its rotation axis chaotically precesses in a sector limited by the solid angle *Q* (see Figure 9*c*). The greater the speed of rectilinear motion of the "electron" core, the more its core flattens along the *X* and *Y* axes (perpendicular to the direction of motion), and the solid angle of the precession sector of its rotation axis decreases. Such shape and behavior of the "electron" core are caused by strong subcont currents in the neck of the toroidal-helical vortex circulating in its outer shell. At a rectilinear motion speed of the "electron" V_z close to the speed of light ($V_z \approx c$), the rotation axis of the "electron" core practically stops precessing and coincides with the direction of its motion.

Nature is fractal, i.e. it is repeated many times on different scales. For example, the movement of an "electron" in a vacuum, of which it itself consists, is similar to the movement of a collared flagellate (an aquatic unicellular organism), which, when moving, causes a toroidal current of water (see Figure 14) [11]. The flagellate is analogous to the compressed core of a moving "electron", and the toroidal movement of water caused by it is similar to a subcont toroidal-helical vortex in the outer shell of a moving "electron".

The rotation of the outer shell of the moving "electron" leads to the emergence of additional inertia of this entire $\lambda_{-12,-16}$-vacuum formation. The faster the "particle" moves, the greater the speed of rotation of its outer shell and, accordingly, the greater the inertia in this rotation. Therefore, it is more difficult to accelerate a moving "particle" even more and it is more difficult to change the direction of its movement.

Due to the conservation laws (which are expressed by Einstein's vacuum equations), if you accelerate the "electron" to a certain speed V_z, then it will continue to move in the $\lambda_{-12,-16}$-vacuum with this speed in the initially given direction.

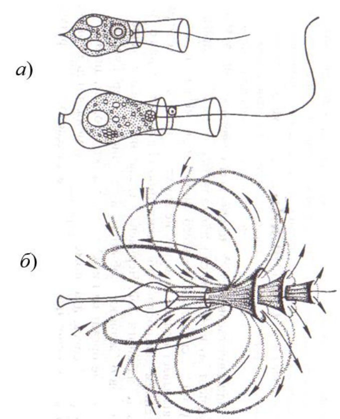

Fig. 14. *a*) Collared flagellates (aquatic unicellular organisms) [11]; *b*) Toroidal water current caused by the movement of the flagellate [11].

6 Accelerations of the antisubcont in the outer shell of a moving "positron"

If with the metrics-solutions of the Einstein vacuum equation (27) – (30)

$$ds_1^{(-a1)2} = -\left(1 - \frac{r_6 r}{\rho}\right)c^2dt^2 + \frac{\rho dr^2}{\Delta^{(a)}} + \rho d\theta^2 + \left(r^2 + a^2 + \frac{r_6 r a^2}{\rho} sin^2\,\theta\right) sin^2\,\theta\, d\phi^2 - \frac{2r_6 ra}{\rho} sin^2\,\theta\, d\phi cdt, \qquad (27')$$

$$ds_2^{(-a2)2} = -\left(1 - \frac{r_6 r}{\rho}\right)c^2dt^2 + \frac{\rho dr^2}{\Delta^{(a)}} + \rho d\theta^2 + \left(r^2 + a^2 + \frac{r_6 r a^2}{\rho} sin^2\,\theta\right) sin^2\,\theta\, d\phi^2 + \frac{2r_6 ra}{\rho} sin^2\,\theta\, d\phi cdt, \qquad (28')$$

$$ds_3^{(-b1)2} = -\left(1 + \frac{r_6 r}{\rho}\right)c^2dt^2 + \frac{\rho dr^2}{\Delta^{(b)}} + \rho d\theta^2 + \left(r^2 + a^2 - \frac{r_6 r a^2}{\rho} sin^2\,\theta\right) sin^2\,\theta\, d\phi^2 - \frac{2r_6 ra}{\rho} sin^2\,\theta\, d\phi cdt, \qquad (29')$$

$$ds_4^{(-b2)2} = -\left(1 + \frac{r_6 r}{\rho}\right)c^2dt^2 + \frac{\rho dr^2}{\Delta^{(b)}} + \rho d\theta^2 + \left(r^2 + a^2 - \frac{r_6 r a^2}{\rho} sin^2\,\theta\right) sin^2\,\theta\, d\phi^2 + \frac{2r_6 ra}{\rho} sin^2\,\theta\, d\phi cdt, \qquad (30')$$

perform actions similar to (56) – (89), then we obtain for the outer shell of the "positron" moving with a constant speed V_z in the direction of the *Z* axis (**Attention!** Calculations should be double-checked):

- components of the vector a_1-antisubcont acceleration $\mathbf{a}^{(-a1)}$

$$a_r^{(-a1)} = a_{Er}^{(-a1)} + a_{Br}^{(-a1)} = -\frac{c^2 r_6 (r^2+a^2-rr_6)(r^2-a^2\cos^2)}{2\left(1-\frac{r_6 r}{r^2+a^2\cos^2\theta}\right)^{\frac{3}{2}}(r^2+a^2\cos^2\theta)^3} + \sqrt{\frac{r_6 r}{r^2+a^2\cos^2\theta}}\,\frac{c^2 r_6 a\sin\theta(a^2\cos^2\theta-r^2)}{(r^2+a^2\cos^2\theta)(r^2+a^2\cos^2\theta-r_6 r)^2}, \quad (106)$$

$$a_\theta^{(-a1)} = a_{E\theta}^{(-a1)} + a_{B\theta}^{(-a1)} = -\frac{c^2 r r_6 a^2\sin 2\theta}{2\left(1-\frac{r_6 r}{r^2+a^2\cos^2\theta}\right)^{\frac{3}{2}}(r^2+a^2\cos^2\theta)^3} + \frac{2c^2 r_6^2 a^2\cos\theta\sin^2\theta(r^2+a^2-r_6 r)}{(r^2+a^2\cos^2\theta)^2(r^2+a^2\cos^2\theta-r_6 r)^2}, \quad (107)$$

$$a_\phi^{(-a1)} = a_{E\phi}^{(-a1)} + a_{B\phi}^{(-a1)} = -\sqrt{\frac{r_6 r}{r^2+a^2\cos^2\theta}}\,\frac{c^2 r_6 a\sin\theta(a^2\cos^2\theta-r^2)}{(r^2+a^2\cos^2\theta)(r^2+a^2\cos^2\theta-r_6 r)^2}; \quad (108)$$

- components of the vector a_2-antisubcont acceleration $\mathbf{a}^{(-a2)}$

$$a_r^{(-a2)} = a_{Er}^{(-a2)} + a_{Br}^{(-a2)} = -\frac{c^2 r_6 (r^2+a^2-rr_6)(r^2-a^2\cos^2)}{2\left(1-\frac{r_6 r}{r^2+a^2\cos^2\theta}\right)^{\frac{3}{2}}(r^2+a^2\cos^2\theta)^3} - \sqrt{\frac{r_6 r}{r^2+a^2\cos^2\theta}}\,\frac{c^2 r_6 a\sin\theta(a^2\cos^2\theta-r^2)}{(r^2+a^2\cos^2\theta)(r^2+a^2\cos^2\theta-r_6 r)^2}, \quad (109)$$

$$a_\theta^{(-a2)} = a_{E\theta}^{(-a2)} + a_{B\theta}^{(-a2)} = -\frac{c^2 r r_6 a^2\sin 2\theta}{2\left(1-\frac{r_6 r}{r^2+a^2\cos^2\theta}\right)^{\frac{3}{2}}(r^2+a^2\cos^2\theta)^3} - \frac{2c^2 r_6^2 a^2\cos\theta\sin^2\theta(r^2+a^2-r_6 r)}{(r^2+a^2\cos^2\theta)^2(r^2+a^2\cos^2\theta-r_6 r)^2}, \quad (110)$$

$$a_\phi^{(-a2)} = a_{E\phi}^{(-a2)} + a_{B\phi}^{(-a2)} = \sqrt{\frac{r_6 r}{r^2+a^2\cos^2\theta}}\,\frac{c^2 r_6 a\sin\theta(a^2\cos^2\theta-r^2)}{(r^2+a^2\cos^2\theta)(r^2+a^2\cos^2\theta-r_6 r)^2}; \quad (111)$$

- components of the vector b_1-antisubcont acceleration $\mathbf{a}^{(-b1)}$

$$a_r^{(-b1)} = a_{Er}^{(-b1)} + a_{Br}^{(-b1)} = -\frac{c^2 r_6 (r^2+a^2-rr_6)(r^2-a^2\cos^2\theta)}{2\left(1+\frac{r_6 r}{r^2+a^2\cos^2\theta}\right)^{\frac{3}{2}}(r^2+a^2\cos^2\theta)^3} + \sqrt{\frac{r_6 r}{r^2+a^2\cos^2\theta}}\,\frac{c^2 r_6 a\sin\theta(a^2\cos^2\theta+r^2)}{(r^2+a^2\cos^2\theta)(r^2+a^2\cos^2\theta-r_6 r)^2}, \quad (112)$$

$$a_\theta^{(-b1)} = a_{E\theta}^{(-b1)} + a_{B\theta}^{(-b1)} = -\frac{c^2 r r_6 a^2\sin 2\theta}{2\left(1+\frac{r_6 r}{r^2+a^2\cos^2\theta}\right)^{\frac{3}{2}}(r^2+a^2\cos^2\theta)^3} + \frac{2c^2 r_6^2 a^2\cos\theta\sin^2\theta(r^2+a^2-r_6 r)}{(r^2+a^2\cos^2\theta)^2(r^2+a^2\cos^2\theta-r_6 r)^2}, \quad (113)$$

$$a_\phi^{(-b1)} = a_{E\phi}^{(-b1)} + a_{B\phi}^{(-b1)} = -\sqrt{\frac{r_6 r}{r^2+a^2\cos^2\theta}}\,\frac{c^2 r_6 a\sin\theta(a^2\cos^2\theta+r^2)}{(r^2+a^2\cos^2\theta)(r^2+a^2\cos^2\theta-r_6 r)^2}; \quad (114)$$

- components of the vector b_2-antisubcont acceleration $\mathbf{a}^{(-b2)}$

$$a_r^{(-b2)} = a_{Er}^{(-b2)} + a_{Br}^{(-b2)} = -\frac{c^2 r_6 (r^2+a^2-rr_6)(r^2-a^2\cos^2)}{2\left(1+\frac{r_6 r}{r^2+a^2\cos^2\theta}\right)^{\frac{3}{2}}(r^2+a^2\cos^2\theta)^3} - \sqrt{\frac{r_6 r}{r^2+a^2\cos^2\theta}}\,\frac{c^2 r_6 a\sin\theta(a^2\cos^2\theta+r^2)}{(r^2+a^2\cos^2\theta)(r^2+a^2\cos^2\theta-r_6 r)^2}, \quad (115)$$

$$a_\theta^{(-b2)} = a_{E\theta}^{(-b2)} + a_{B\theta}^{(-b2)} = -\frac{c^2 r r_6 a^2\sin 2\theta}{2\left(1+\frac{r_6 r}{r^2+a^2\cos^2\theta}\right)^{\frac{3}{2}}(r^2+a^2\cos^2\theta)^3} - \frac{2c^2 r_6^2 a^2\cos\theta\sin^2\theta(r^2+a^2-r_6 r)}{(r^2+a^2\cos^2\theta)^2(r^2+a^2\cos^2\theta-r_6 r)^2}, \quad (116)$$

$$a_\phi^{(-b2)} = a_{E\phi}^{(-b2)} + a_{B\phi}^{(-b2)} = \sqrt{\frac{r_6 r}{r^2+a^2\cos^2\theta}}\,\frac{c^2 r_6 a\sin\theta(a^2\cos^2\theta+r^2)}{(r^2+a^2\cos^2\theta)(r^2+a^2\cos^2\theta-r_6 r)^2}. \quad (117)$$

The general vector field of accelerated antisubcont currents in the outer shell of a “positron” moving rectilinearly and uniformly (i.e. with a constant velocity V_z) in the direction of the Z axis is determined by the vector-quaternion

$$\mathbf{a}_{\Sigma}^{(-ab)} = \frac{1}{4}\left(\mathbf{a}^{(-a1)} + i\mathbf{a}^{(-a2)} + j\mathbf{a}^{(-b1)} + k\mathbf{a}^{(-b2)}\right), \qquad (118)$$

where

$\mathbf{a}^{(-a1)} = \mathbf{E}_o^{(-a1)} + [\mathbf{v}^{(-a1)} \times \mathbf{B}_o^{(-a1)}]$ is vector field of accelerations of a_1-antisubcont (106) – (108); (119)

$\mathbf{a}^{(-a2)} = \mathbf{E}_o^{(-a2)} + [\mathbf{v}^{(-a2)} \times \mathbf{B}_o^{(-a2)}]$ is vector field of accelerations of a_2-antisubcont (109) – (111);

$\mathbf{a}^{(-b1)} = \mathbf{E}_o^{(-b1)} + [\mathbf{v}^{(-b1)} \times \mathbf{B}_o^{(-b1)}]$ is vector field of accelerations of b_1-antisubcont (112) – (114);

$\mathbf{a}^{(-b2)} = \mathbf{E}_o^{(-b2)} + [\mathbf{v}^{(-b2)} \times \mathbf{B}_o^{(-b2)}]$ is vector field of accelerations of b_2-antisubcont (115) – (117).

The components of the a_k- and b_k-antisubcont acceleration vectors (106) – (117) in the outer shell of the moving “positron” are completely opposite to the corresponding components of the a_k- and b_k-subcont acceleration (90) – (98) in the outer shell of the moving “electron”. That is, the difference between the corresponding components (90) – (98) and (106) – (117) is zero.

This means that all laminar (rectilinear) and turbulent (rotational) antisubcont flows in the outer shell of the moving “positron” are completely opposite to the corresponding laminar and turbulent subcont flows in the outer shell of the “electron” moving with the same speed and in the same direction (see Figure 15). In addition, the "positron" and "electron" are rotated (or phase-shifted) by 90^0 relatives to each other (see §5.2 in [3]).

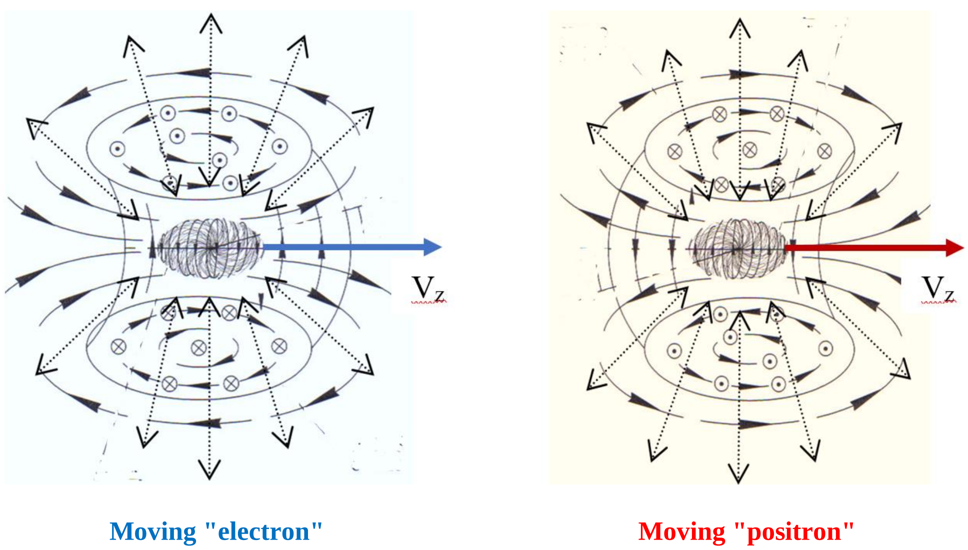

Fig. 15. "Electron" and "positron" moving rectilinearly and uniformly with the same speed V_z in the same direction. In this case, all processes (i.e. accelerated laminar and turbulent flows) in their outer shells are mutually opposite

If the "electron" and "positron" move rectilinearly and uniformly with the same speed V_z, but in opposite directions, then all processes (i.e. accelerated laminar and turbulent flows) in their outer shells completely coincide (see Figure 16). In this case, they are practically indistinguishable.

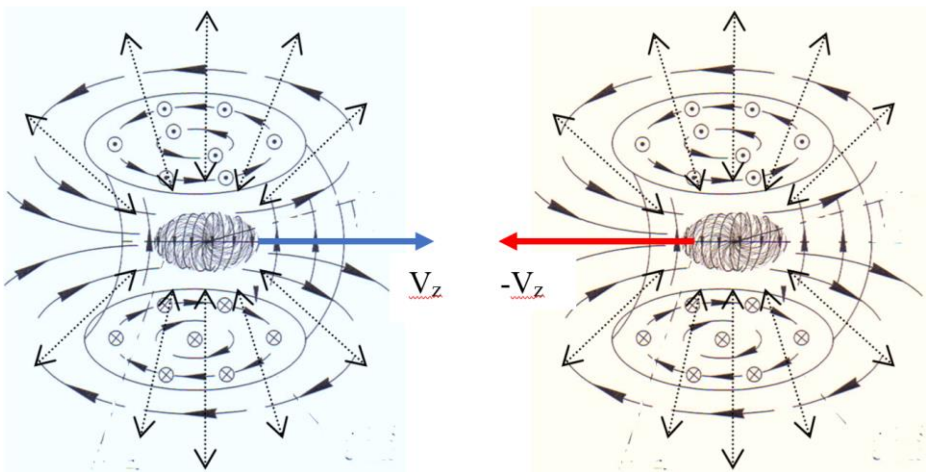

Moving "electron" Moving "positron"

Fig. 16. "Electron" and "positron" moving rectilinearly and uniformly with the same speed V_z, but in opposite directions. In this case, all processes (i.e. accelerated laminar and turbulent flows) in their outer shells completely coincide

7 Outer shell of the moving "proton"

The motion of the "proton" and "antiproton", "neutron", hydrogen "atom" and other particles, the metric-dynamic models of which were considered in §4 in [6], requires a separate study.

In this article, as an example, we will only present a multilayer metric-dynamic model of the outer shell of one of the possible states of the p_1-"proton" (92) in [6]

$$\begin{array}{l} d_r^{+}(+\ +\ +\ -) \\ u_g^{-}(-\ +\ -\ +) \\ u_b^{-}\underline{(-\ -\ +\ +)} \\ p_1^{-}(-\ +\ +\ +)_{+} \end{array} \qquad (120)$$

which moves rectilinearly and uniformly with constant velocity V_z in the vacuum of which it itself consists

p_1^--"PROTON" (121)

moving rectilinearly and uniformly.

Outer shell with averaged signature (– + + +)

Outer shell of the moving valence d_r^+-"quark",

in the interval $[r_4, r_6]$, signature (+ + + –)

$$ds_1^{(-a1)2} = \left(1 - \frac{r_6 r}{\rho}\right) c^2dt^2 + \frac{\rho dr^2}{\Delta^{(a)}} + \rho d\theta^2 - \left(r^2 + a^2 + \frac{r_6 r a^2}{\rho} sin^2\,\theta\right) sin^2\,\theta\, d\phi^2 - \frac{2r_6 r a}{\rho} sin^2\,\theta\, d\phi c dt, \qquad (122)$$
$$ds_2^{(-a2)2} = \left(1 - \frac{r_6 r}{\rho}\right) c^2dt^2 + \frac{\rho dr^2}{\Delta^{(a)}} + \rho d\theta^2 - \left(r^2 + a^2 + \frac{r_6 r a^2}{\rho} sin^2\,\theta\right) sin^2\,\theta\, d\phi^2 + \frac{2r_6 r a}{\rho} sin^2\,\theta\, d\phi c dt,$$
$$ds_3^{(-b1)2} = \left(1 + \frac{r_6 r}{\rho}\right) c^2dt^2 + \frac{\rho dr^2}{\Delta^{(b)}} + \rho d\theta^2 - \left(r^2 + a^2 - \frac{r_6 r a^2}{\rho} sin^2\,\theta\right) sin^2\,\theta\, d\phi^2 - \frac{2r_6 r a}{\rho} sin^2\,\theta\, d\phi c dt,$$
$$ds_4^{(-b2)2} = \left(1 + \frac{r_6 r}{\rho}\right) c^2dt^2 + \frac{\rho dr^2}{\Delta^{(b)}} + \rho d\theta^2 - \left(r^2 + a^2 - \frac{r_6 r a^2}{\rho} sin^2\,\theta\right) sin^2\,\theta\, d\phi^2 + \frac{2r_6 r a}{\rho} sin^2\,\theta\, d\phi c dt;$$

Outer shell of the moving valence u_g^--"quark",

in the interval $[r_4, r_6]$, signature (– + – +)

$$ds_5^{(-a3)2} = -\left(1-\frac{r_6 r}{\rho}\right)c^2dt^2 + \frac{\rho dr^2}{\Delta^{(a)}} - \rho d\theta^2 + \left(r^2 + a^2 + \frac{r_6 r a^2}{\rho}\sin^2\theta\right)\sin^2\theta\, d\phi^2 - \frac{2r_6 ra}{\rho}\sin^2\theta\, d\phi c dt, \quad (123)$$

$$ds_6^{(-a4)2} = -\left(1-\frac{r_6 r}{\rho}\right)c^2dt^2 + \frac{\rho dr^2}{\Delta^{(a)}} - \rho d\theta^2 + \left(r^2 + a^2 + \frac{r_6 r a^2}{\rho}\sin^2\theta\right)\sin^2\theta\, d\phi^2 + \frac{2r_6 ra}{\rho}\sin^2\theta\, d\phi c dt,$$

$$ds_7^{(-b3)2} = -\left(1+\frac{r_6 r}{\rho}\right)c^2dt^2 + \frac{\rho dr^2}{\Delta^{(b)}} - \rho d\theta^2 + \left(r^2 + a^2 - \frac{r_6 r a^2}{\rho}\sin^2\theta\right)\sin^2\theta\, d\phi^2 - \frac{2r_6 ra}{\rho}\sin^2\theta\, d\phi c dt,$$

$$ds_8^{(-b4)2} = -\left(1+\frac{r_6 r}{\rho}\right)c^2dt^2 + \frac{\rho dr^2}{\Delta^{(b)}} - \rho d\theta^2 + \left(r^2 + a^2 - \frac{r_6 r a^2}{\rho}\sin^2\theta\right)\sin^2\theta\, d\phi^2 + \frac{2r_6 ra}{\rho}\sin^2\theta\, d\phi c dt;$$

Outer shell of the moving valence u_b^--"quark"

in the interval $[r_4, r_6]$, signature (– – + +)

$$ds_9^{(-a5)2} = -\left(1-\frac{r_6 r}{\rho}\right)c^2dt^2 - \frac{\rho dr^2}{\Delta^{(a)}} + \rho d\theta^2 + \left(r^2 + a^2 + \frac{r_6 r a^2}{\rho}\sin^2\theta\right)\sin^2\theta\, d\phi^2 - \frac{2r_6 ra}{\rho}\sin^2\theta\, d\phi c dt, \quad (124)$$

$$ds_{10}^{(-a6)2} = -\left(1-\frac{r_6 r}{\rho}\right)c^2dt^2 - \frac{\rho dr^2}{\Delta^{(a)}} + \rho d\theta^2 + \left(r^2 + a^2 + \frac{r_6 r a^2}{\rho}\sin^2\theta\right)\sin^2\theta\, d\phi^2 + \frac{2r_6 ra}{\rho}\sin^2\theta\, d\phi c dt,$$

$$ds_{11}^{(-b5)2} = -\left(1+\frac{r_6 r}{\rho}\right)c^2dt^2 - \frac{\rho dr^2}{\Delta^{(b)}} + \rho d\theta^2 + \left(r^2 + a^2 - \frac{r_6 r a^2}{\rho}\sin^2\theta\right)\sin^2\theta\, d\phi^2 - \frac{2r_6 ra}{\rho}\sin^2\theta\, d\phi c dt,$$

$$ds_{12}^{(-b6)2} = -\left(1+\frac{r_6 r}{\rho}\right)c^2dt^2 - \frac{\rho dr^2}{\Delta^{(b)}} + \rho d\theta^2 + \left(r^2 + a^2 - \frac{r_6 r a^2}{\rho}\sin^2\theta\right)\sin^2\theta\, d\phi^2 + \frac{2r_6 ra}{\rho}\sin^2\theta\, d\phi c dt;$$

The substrate of p_1^--"proton"

uniformly and rectilinearly moving,

$r \in [0, \infty]$, signature (– + + +)

$$ds_{13}^{(-)2} = -c^2dt^2 + \frac{\rho dr^2}{r^2+a^2} + \rho d\theta^2 + (r^2+a^2)\sin^2\theta\, d\phi^2. \quad (125)$$

At $V_z = 0$ (i.e., in the absence of motion), metrics (122) – (125) acquire the original form (93) – (95) in [6].

The methods for extracting information about the deformations, velocities, and accelerations of the subcont in the outer shell of a moving p_1^--"proton" are shown using the example of a moving "electron" (see §§2–5 of this article). However, the volume of calculations in this case increases more than threefold.

8 Outer shell of a moving "quark"

In this article, we have considered in detail only the metric-dynamic models of the outer shells of a moving "electron" and a moving "positron". However, the methods of extracting information from metrics (21) – (25) and (27) – (31) are suitable for describing the similar behavior of outer shells during the motion of all stable and unstable spherical vacuum formations considered in §4 in [6]: "quarks", "baryons" and "mesons".

For example, the metric-dynamic model of the outer shell of a moving u_r^--"antiquark" (71) in [6] with the signature (– + + –) is determined by the metrics

The outer shell of a moving valence u_r^--"antiquark"

in the interval $[r_4, r_6]$, signature (– + + –)

$$ds_1^{(-a1)2} = -\left(1-\frac{r_6 r}{\rho}\right)c^2dt^2 + \frac{\rho dr^2}{\Delta^{(a)}} + \rho d\theta^2 - \left(r^2 + a^2 + \frac{r_6 r a^2}{\rho}\sin^2\theta\right)\sin^2\theta\, d\phi^2 - \frac{2r_6 ra}{\rho}\sin^2\theta\, d\phi c dt, \quad (126)$$

$$ds_2^{(-a2)2} = -\left(1-\frac{r_6 r}{\rho}\right)c^2dt^2 + \frac{\rho dr^2}{\Delta^{(a)}} + \rho d\theta^2 - \left(r^2 + a^2 + \frac{r_6 r a^2}{\rho}\sin^2\theta\right)\sin^2\theta\, d\phi^2 + \frac{2r_6 ra}{\rho}\sin^2\theta\, d\phi c dt,$$

$$ds_3^{(-b1)2} = -\left(1+\frac{r_6 r}{\rho}\right)c^2dt^2 + \frac{\rho dr^2}{\Delta^{(b)}} + \rho d\theta^2 - \left(r^2 + a^2 - \frac{r_6 r a^2}{\rho}\sin^2\theta\right)\sin^2\theta\, d\phi^2 - \frac{2r_6 ra}{\rho}\sin^2\theta\, d\phi c dt,$$

$$ds_4^{(-b2)2} = -\left(1+\frac{r_6 r}{\rho}\right)c^2dt^2 + \frac{\rho dr^2}{\Delta^{(b)}} + \rho d\theta^2 - \left(r^2 + a^2 - \frac{r_6 r a^2}{\rho}\sin^2\theta\right)\sin^2\theta\, d\phi^2 + \frac{2r_6 ra}{\rho}\sin^2\theta\, d\phi c dt;$$

The substrate of u_r^--"antiquark"

uniformly and rectilinearly moving, $r \in [0, \infty]$, signature (– + + –)

$$ds_5^{(-)2} = -c^2dt^2 + \frac{\rho dr^2}{r^2+a^2} + \rho d\theta^2 - (r^2+a^2)\sin^2\theta\, d\phi^2. \quad (127)$$

Similarly, metric-dynamic models of the outer shells of all moving colored "quarks" given in Table 1 in [6] can be specified. In this case, metric-dynamic models of the outer shells of all these 16 "quarks" are determined by sets of metrics (126) - (127) with the corresponding signature from Table 1 in [6]. In turn, from these 16 "quarks" metric-dynamic models of all elements of the Standard Model of elementary "particles" moving rectilinearly and uniformly can be composed.

9 Condition of annihilation of "particles" and "antiparticles"

In the previous paragraphs it was shown that the outer shells of all moving stable spherical vacuum formations, such as: "electrons" and "positrons", "protons" and "antiprotons", "neutrons" and "antineutrons", "mesons" and "antimesons", etc., considered in §4 in [6], are described similarly. For example, despite the fact that the "proton" consists of three valence "quarks", during its translational motion around its core, on average, laminar and turbulent antisubcont currents are induced, similar to the antisubcont accelerated currents arising during the motion of the "positron". Only the metric-dynamic model of a moving "proton" is significantly more complex, since it does not consist of 4 Kerr metrics (27) – (30) with a signature $(- + + +)$, but of $3 \times 4 = 12$ similar metrics, for example, (122) – (124) with signatures from the ranking (120).

In the framework of the geometrized vacuum physics (GVPh, see [1,2,3,4,5,6,7]) developed here, all bodies consist of "particles" and "antiparticles" that do not annihilate, since they are very complexly mixed, intertwined with each other and are constantly in thermal chaotic motion. In other words, "particles" and "antiparticles" in bodies are so complexly tied into topological (i.e. signature) nodes and move so complexly with the induction of toroidal-helical vacuum currents that it is practically impossible to untangle them. But mobile free "particles" and "antiparticles" (in particular, moving "electrons" and "positrons") cannot annihilate, since for mutual destruction they must completely coincide with each other. For example, if you tear a piece of fabric out of a tablecloth, it is almost impossible to completely restore the integrity of the tablecloth, since the torn piece of fabric will never perfectly fill the hole.

Presumably, the annihilation of slow "particles" and "antiparticles" (in particular, the "electron" and "positron") is possible only when they are practically at rest. Only after the "particle" and "antiparticle" have practically come to a complete stop can the spiral-rotational approach (i.e. the dance of death, see Figure 17) begin. During the annihilation of a "particle" and "antiparticle", their cores circle around each other for so long until they emit (i.e. throw off in the form of radiation) all that is superfluous, and coincide with each other with absolute precision (i.e. the convexity of the vacuum must fill its concavity with the highest precision). Thus, the annihilation of "particles" and "antiparticles" inside bodies, where they are tightly packed, complexly mixed and constantly participate in thermal (chaotic) motion, is practically impossible.

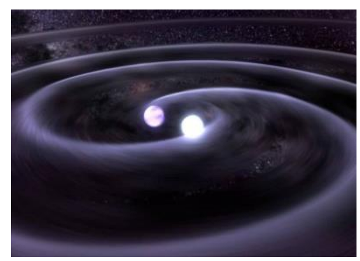

Fig. 17. The dance of death

Thus, it should be expected that the process of annihilation of "particles" and "antiparticles" (i.e. their dance of death) can begin only when they are practically at rest relative to each other and the surrounding vacuum, of which they themselves are stable deformations (i.e. when they shed the excess rotational inertia associated with their motion). In other words, atomic bodies can self-annihilate (with the release of enormous energy) at a temperature close to absolute zero. It is estimated that the process of self-annihilation of an atomic body can begin at its temperature of 0.08 – 0.3 K.

10 Geometrized model of motion of bodies by inertia

When an atomic body moves as a whole, the "particles" and "antiparticles" that fill it move in one direction. In this case, toroidal-helical vortices (geometrized magnetic fields) are induced around their cores. But these vortices are mutually opposite in "particles" and "antiparticles" (see Figures 15 and 18), so these vacuum rotations, on average, compensate each other's manifestations. As a result, a general geometrized magnetic field is not observed around the moving body. In other words, mutually opposite magnetic fields (i.e., rotational accelerations of the subcont and antisubcont around the direction of motion of the moving cores of "particles" and "antiparticles") are constantly induced when the body moves in a vacuum, but on average, they almost completely compensate each other's manifestations.

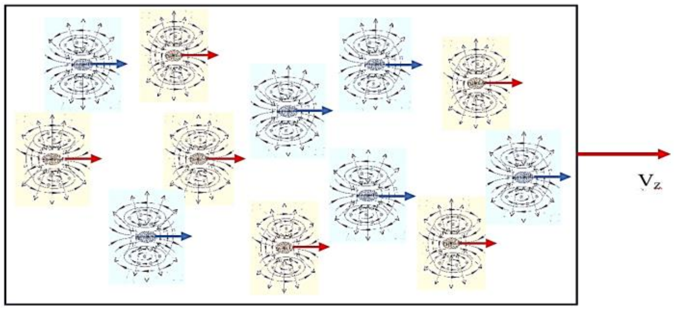

Fig. 18. "Particles" and "antiparticles" (in particular "electrons" and "positrons") moving along with the entire body rectilinearly and uniformly with the same speed V_z

Thus, in order for the body to start moving, part of the force applied to it is spent on inducing toroidal-helical vacuum vortices (geometrized magnetic fields) in the direction of its motion. However, due to the fact that "particles" and "antiparticles" induce mutually opposite vacuum vortices, the general magnetic field around the moving body is present, but does not manifest itself, since the effect of counter vortices and anti-vortices is mutually compensated.

The expenditure of external forces on inducing mutually opposite toroidal-helical vortices (geometrized magnetic fields) is the cause of the inertia of bodies, i.e. resistance to the onset of motion. However, if the body is already set in rectilinear and uniform motion, then the mutually opposite toroidal-helical vortices induced in this case will support the motion of the body in the same direction and at the same speed, since these two counter rotations are preserved, as evidenced by the stationarity of the Kerr metrics (21) – (24) and (27) – (30). Within the framework of the GVPh, this is the reason for the infinite motion of bodies in a vacuum by inertia.

On the contrary, forced braking of a moving body is accompanied by resistance from the inertia of mutually opposite toroidal-helical vacuum vortices. The preservation of mutually opposite rotation of the vacuum around a moving body does not allow this body to be braked instantly. For the same reason, it is not easy to change the direction of its motion.

The explanation of the motion of bodies by inertia proposed by GFV due to the induction of mutually opposite toroidal-helical vacuum vortices (counter geometrized magnetic fields) allows one to completely get rid of the concept of the inertial mass of a body. In other words, the proposed mechanism for the emergence of inertia due to the induction of mutually opposite rotational vacuum flows around a moving body is, in essence, a geometrization of the concept of mass. In this case, the more interconnected "particles" and "antiparticles" participate in the collective (joint) motion (i.e. the more "particles" and "anti-particles" in the body, see Figure 18), the more counter toroidal-helical vortices are induced around their nuclei and the greater the general inertia of such a body. This is equivalent to an increase in the mass of the body with an increase in the number of atoms and molecules.

11 Inertioid (practical application of inertial metrodynamics)

The metric-dynamic model of the interaction of a moving body with the surrounding vacuum, developed on the basis of solutions of the Einstein vacuum equation, can be used for the theoretical justification of the occurrence of thrust in mechanisms such as Tolchin's inecioids (see Figure 19).

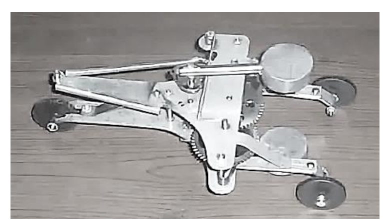

Fig. 19. Implementation of one of several variants of constructing Tolchin inertioids

From the point of view of Geometrized vacuum physics, inertioids should be considered not as closed, but as open mechanical systems interacting with a vacuum [12]. That is, it is possible to push off from a vacuum during the accelerated motion of the inertioid flywheels.

The use of inertioids on spacecraft can contribute to the development of a method for correcting the orbit of satellites in a vacuum that does not require a large consumption of fuel from jet engines to correct their orbit. This could lead to significant savings and extend the service life of spacecraft.

12 Counter "electron" - "positron" electric current

In modern physics, it is generally accepted that electric current is a directed movement of charged particles. In particular, it is assumed that electrons are the carriers of electric charge in metals.

In Geometrized vacuum physics (GVPh) there is no asymmetry between "particles" and "antiparticles", so we are forced to state that electric current is a counter-directed movement of "particles" and "antiparticles".

It should be noted that the counter current of particles and antiparticles is not news. For example, it is believed that electron-hole conductivity occurs in semiconductors. It is simply due to the established scientific paradigm that "positrons" were called "holes".

Within the framework of the GVPh, during the counter motion of, for example, “electrons” and “positrons” in a metal wire (see Figure 20):
- firstly, “particles” and “antiparticles” cannot annihilate, for the reasons indicated in §9;
- secondly, toroidal-helical vortices (i.e. geometrized magnetic fields) induced around the nuclei of “particles” and “antiparticles” moving towards each other rotate in the same direction (see Figures 16 and 20*a*).

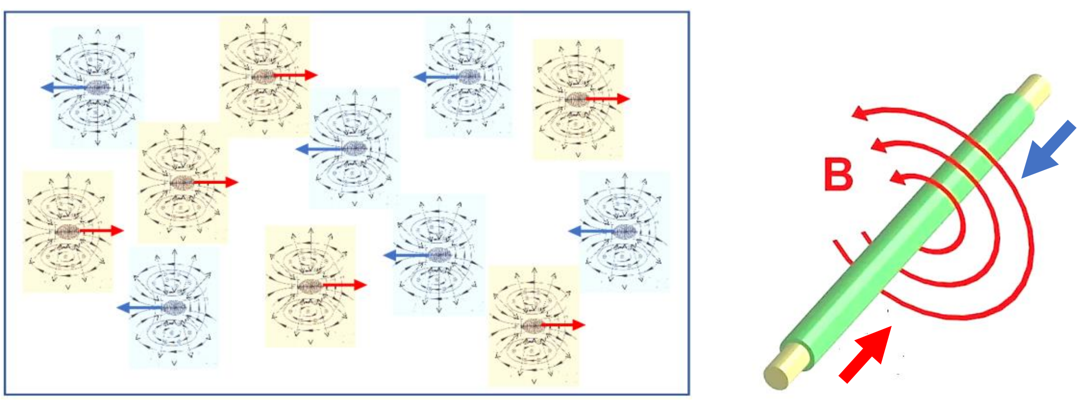

a) *b*)

Fig. 20. "Particles" and "antiparticles" (in particular, "electrons" and "positrons") moving in a metal wire rectilinearly and uniformly with the same speed V_z towards each other, i.e. in opposite directions. At the same time, their counter toroidal-helical vortices rotate in one direction

As a result, a joint geometrized magnetic field is induced around the conductor with a counter "electron" - "positron" current (see Figure 20*b*), i.e., an averaged rotation of the vacuum.

CONCLUSION

This part of the Geometrized vacuum physics (GVPh) proposes metric-dynamic models of the outer shells of moving "particles" (in particular, moving "electron" and moving "positron"), provided that they move rectilinearly and uniformly (i.e. with a constant velocity V_z) in the direction of the Z axis relative to the vacuum, of which they themselves are stable curvatures.

These metric-dynamic models of the outer shells consist of sets of Kerr metrics with different signatures: (21) – (25) for a moving "electron" with the signature (+ – – –); (27) – (31) for a moving "positron" with the signature (– + + +); (122) – (125) for a moving "proton" with signatures (120); (126) – (127) for a moving u_r-“antiquark” with the signature (– + + –).

Metrics-solutions with common (or averaged) signatures (+ – – –) and (– + + +) are exact solutions of the Einstein vacuum equation (42) in [5] ($R_{ik} = 0$), which is essentially a mathematical expression of conservation laws (see [5,6]). This means that “particles” moving relative to a vacuum at rest rectilinearly and uniformly (i.e. with a constant velocity) remain in this unchanged state until they are subjected to a braking effect.

As a result of the analysis of the sets of metrics-solutions (21) – (25) for the moving "electron" and (27) - (31) for the moving "positron" using the methods of the GVPh and the Algebra of signature described in [1,2,3,4,5,6.7], the following main results were obtained. With rectilinear and uniform motion of the valence "electron" and valence "positron" relative to the vacuum of which they consist:

1) the averaged outer shell of the valence "electron" takes the form of an ellipsoid of revolution, flattened along the Z axis, which coincides with the direction of its motion (see Figure 4);
2) the averaged lines of force of the geometrized electric field (i.e. the field of laminar accelerations of the subcont) in the outer shell of the valence "electron" are compressed (see Figure 13a,b);
3) the core of the moving valence "electron" (or "positron") is compressed along the Y and X axes, perpendicular to the direction of motion, and acquires the shape of an elongated spheroid (olive), the axis of rotation of which chaotically precesses in a limited sector (see Figure 13c);
4) two counter toroidal-helical vortices of the subcont are induced around the moving core of the "electron" (or "positron") (i.e., on average, a completely compensated geometrized magnetic field, or an averaged field of turbulent accelerations of the subcont) (see Figure 7, or Figure 8);
5) similar metamorphoses occur with the moving "positron" as with the moving "electron", but all processes in the outer shell of the "positron" proceed in the opposite direction to the processes occurring in the outer shell of the "electron".

In this article we have considered in detail only the metric-dynamic models of the outer shells of the moving "electron" and the moving "positron". However, the methods of extracting information from the metrics (21) – (25) and (27) – (31) are suitable for describing the similar behavior of the outer shells during the motion of all stable and unstable spherical vacuum formations considered in §4 in [6]: "quarks", "baryons", "mesons".

When choosing the model of a moving "electron" relative to the vacuum, of which it is a stable curvature, we proceeded from how stable disturbances move in atomistic media (see, for example, see Figures 1 and 10). This is based on the belief that similarity is one of the principles of formation of natural objects. This belief is supported by the presence of Kerr metrics – as exact solutions of Einstein's vacuum equations. This heuristic approach does not seem convincing, but the metric-dynamic models of moving “particles” and “antiparticles” proposed here allow us to describe geometrically the following fundamental phenomena:

1) Electromagnetic fields around moving “particles” and “antiparticles” within the framework of the GVPh can be represented as completely geometrized vector fields of laminar (linear) and turbulent (rotational) accelerations of various layers of vacuum.

2) It is possible to explain the inert properties of bodies consisting of "particles" and "antiparticles". When such a body moves relative to a stationary vacuum, then mutually opposite toroidal-helical vacuum vortices (i.e. geometrized magnetic fields) are induced around the "particles" and "antiparticles" (see Figures 15 and 18). In order for these vortices to arise, it is necessary to expend effort, which explains the resistance of the body to the transition from a state of rest relative to the vacuum to a state of its rectilinear and uniform motion. When counter toroidal-helical vacuum vortices are induced, they support the motion of "particles" and "antiparticles" and the entire atomic body as a whole with a constant speed, since the integral rotational acceleration of the vacuum is preserved. To stop a body moving relative to a vacuum, it is necessary to expend effort to stop the induced counter toroidal-helical vortices. At the same time, the geometrized magnetic field of a moving body does not manifest itself, since the toroidal-helical vortices of the "particles" are compensated by the opposite toroidal-helical vortices of the "antiparticles". The greater the speed of the joint translational motion V_z of the "particles" and "antiparticles" (in particular, "electrons" and "positrons") of the body, the more intensively the toroidal-helical vortices of the vacuum twist around the direction of motion. In addition, for example, the toroidal-helical vortices of the antisubcont, induced around the moving

nucleus of the "proton" are significantly more complex and more difficult to induce, since it consists not of one, but of those "quarks" (see §7). Taken together, all these properties of a moving body as a set of "particles" and "antiparticles" (in particular, "electrons" - "positrons", "protons" - "antiprotons", "neutrons" - "antineutrons", etc.) completely explain its inert properties in terms of counter-accelerated rotational accelerations of various vacuum layers (subcont and antisubcont) induced around their nuclei. In other words, it is possible to completely hermetically seal the explanation of the inert properties of atomic bodies without invoking the vague concept of "inert mass".

3) In the framework of the GVPh, electric current is a directed counter-movement of "particles" and "antiparticles" (in particular, "electrons" and "positrons"). In this case, when stable mutually opposite vacuum formations move towards each other, the directions of their toroidal-helical subcont-antisubcont currents coincide (see Figure 16 and 20). As a result, the general (average) movement of, for example, a metal conductor is absent, and a general geometrized magnetic field is induced around the conductor (i.e., a looped field of rotational accelerations of the vacuum, see Figure 20b). Thus, such a phenomenon as electric current can be explained from the standpoint of geometrized (inert) metro-dynamics.

4) In the GVPh developed here, we are forced to assume that "particles" and "antiparticles" in atomic bodies cannot annihilate because they are constantly in thermal motion, while counter toroidal-helical vortices are constantly induced around them, which support their coexistence, since the inertia of rotation of the vacuum around the moving nuclei cannot be eliminated. Therefore, the article suggests that the annihilation of atomic bodies consisting of "particles" and "antiparticles" is possible only at temperatures close to absolute zero (i.e., approximately at 0.08 – 0.3 K). Thus, if atomic bodies are completely frozen, then upon their disappearance, a colossal amount of accelerated motion (wave disturbances) of the vacuum will be released.

This article is devoted to the geometrization of processes and phenomena at the picoscopic level of existence (i.e. at the level of elementary "particles"). However, as has been repeatedly noted in [1,2,3,4,5,6.7], the metrodynamics of the GVPh is universal for all scales of consideration. If in all the equations of this article instead of $r_6 \sim 10^{-13}$ cm (the radius of the core of an elementary "particle", in particular the nucleus of an "electron") we substitute any other radius from the hierarchy (44a) in [6].

$r_1 \sim 10^{39}$ cm is radius commensurate with the radius of the mega-Universe;

$r_2 \sim 10^{29}$ cm is radius commensurate with the radius of the observable Universe;

$r_3 \sim 10^{19}$ cm is radius commensurate with the radius of the galactic core;

$r_4 \sim 10^{8}$ cm is radius commensurate with the radius of the core of a planet or star;

$r_5 \sim 10^{-3}$ cm is radius commensurate with the radius of a biological cell;

$r_6 \sim 10^{-13}$ cm is radius commensurate with the radius of an elementary particle core;

$r_7 \sim 10^{-24}$ cm is radius commensurate with the radius of a proto-quark core;

$r_8 \sim 10^{-34}$ cm is radius commensurate with the radius of a plankton core;

$r_9 \sim 10^{-45}$ cm is radius commensurate with the radius of the proto-plankton core;

$r_{10} \sim 10^{-55}$ cm is radius commensurate with the size of the instanton core,

then we get a geometrized description of the behavior of the vacuum in the outer shells of the "proto-quarks" ($r_7 \sim 10^{-24}$ cm), or "planets" ($r_7 \sim 10^{-24}$ см cm), or "galaxies" ($r_3 \sim 10^{19}$ cm), etc.

All formulas presented in this article should be rechecked by mathematicians who have the skills to automate calculations using specialized software. I offer cooperation to specialists who are able to create an interactive model of moving "particles" based on the mathematical apparatus proposed here.

In the author's opinion, despite possible shortcomings, this article has made another step towards completing the Clifford-Einstein-Wheeler program for the complete geometrization of physics.

ACKNOWLEDGEMENTS

I sincerely thank Gavriel Davidov, David Reid, Tatyana Levy, Eliezer Rahman and David Kogan, Gennady Ivanovich Shipov, Carlos J. Rojas, Alexander Maslov and Alexander Bolotov, Alexander Bindiman for their assistance. I thank David Johnson for providing an overview of the helical-toroidal electron concept.

REFERENCES

[1] Batanov-Gaukhman, M. (2023). Geometrized Vacuum Physics. Part I. Algebra of Stignatures. Avances en Ciencias e Ingeniería, 14 (1), 1-26, https://www.executivebs.org/publishing.cl/avances-en-ciencias-e-ingenieria-vol-14-nro-1-ano-2023-articulo-1/ ; and viXra:2403.0035, and Preprints, 2023060765. https://doi.org/10.20944/preprints202306.0765.v3, Available in Russian: https://doi.org/10.24108/preprints-3113027.

[2] Batanov-Gaukhman, M. (2023). Geometrized Vacuum Physics. Part II. Algebra of Signatures. Avances en Ciencias e Ingeniería, 14 (1), 27-55, https://www.executivebs.org/publishing.cl/avances-en-ciencias-e-ingenieria-vol-14-nro-1-ano-2023-articulo-2/: and Preprints, 2023070716, https://doi.org/10.20944/preprints202307.0716.v1. and viXra:2403.0034. Available in Russian: https://doi.org/10.24108/preprints-3113028.

[3] Batanov-Gaukhman, M. (2023). Geometrized Vacuum Physics. Part III. Curved Vacuum Area. Avances en Ciencias e Ingeniería Vol. 14 nro 2 año 2023 Articulo 5, https://www.executivebs.org/publishing.cl/avances-en-ciencias-e-ingenieria-vol-14-nro-2-ano-2023-articulo-5/; and Preprints 2023, 2023080570. https://doi.org/10.20944/preprints202308.0570.v4. and viXra:2403.0033. Available in Russian: https://doi.org/10.24108/preprints-3113032.

[4] Batanov-Gaukhman, M. (2024). Geometrized Vacuum Physics. Part IV: Dynamics of Vacuum Layers. Avances en Ciencias e Ingeniería Vol. 14 nro 3 año 2023 Articulo 1 https://www.executivebs.org/publishing.cl/avances-en-ciencias-e-ingenieria-vol-14-nro-3-ano-2023-articulo-1/, and Preprints.org. https://doi.org/10.20944/preprints202310.1244.v3. and viXra:2403.0032 . Available in Russian: https://doi.org/10.24108/preprints-3113039.

[5] Batanov-Gaukhman, M. (2024). Geometrized Vacuum Physics Part 5: Stable Vacuum Formations. Avances en Ciencias e Ingeniería Vol. 14 nro 3 año 2023 Articulo 2 https://www.executivebs.org/publishing.cl/avances-en-ciencias-e-ingenieria-vol-14-nro-3-ano-2023-articulo-2/ and viXra:2405.0002. Available in Russian: https://doi.org/10.24108/preprints-3113040.

[6] Batanov-Gaukhman, M. (2024). Geometrized Vacuum Physics Part 6: Hierarchical Cosmological Model, Avances en Ciencias e Ingeniería Vol. 14 nro 4 año 2023 Articulo 3. https://www.executivebs.org/publishing.cl/avances-en-ciencias-e-ingenieria-vol-14-nro-4-ano-2023-articulo-3/ and viXra:2408.0010. Available in Russian: https://doi.org/10.24108/preprints-3113086.

[7] Batanov-Gaukhman, M. (2024). Geometrized Vacuum Physics Part 7: "Electron" and "Positron", viXra:2409.0097. Available in Russian: https://doi.org/10.24108/preprints-3113132.

[8] Vladimirov, Yu.S. (2005). Geometrophysics. – Moscow: Binom.

[9] Korn, G. & Korn, T. (1984). Handbook of Mathematics, – M.: Science.

[10] Detlaff, A.A. Yavorsky B.M. (2014). Course of Physics, – M.: Academia ISBN: 9785446804702.

[11] Dogel, V.A. (1981). Zoology of Invertebrates. – Moscow: Higher School.

[12] Shipov, G. (1998). The Theory of Physical Vacuum. – Moscow ST-Center, Russia ISBN 5 7273-0011-8.

[13] Cambier, J. & Micheletti, D. (2000). Theoretical Analysis of the Electron Spiral Toroid Concept// MSE Technology Applications, Inc., Butte, Montan /NASA/CR-2000-210654.

[14] Chen, C.; Pakter, R.; Seward, D. (2001). Equilibrium and Stability Properties of Self-Organized Electron Spiral Toroids// Physics of Plasmas, DOI:10.1063/1.1400792, Corpus ID: 122229306.

[15] Consa, O. (2017). G-factor and the Helical Solenoid Electron Model. viXra:1702.0185.

[16] Consa, O. (2018). Helical Solenoid Model of the Electron. Progress in Physics, 14, 80-89.

[17] Williamson, J. & Van der Mark, M. (1997) Is the Electron a Photon with Toroidal Topology? Annales de la Fondation Louis de Broglie, v. 22, 133–146.

[18] Kyriakos, A. (2004). Geometrical Illustration of the Electromagnetic Representation of Dirac's Electron Theory. ArXiv: quant-ph/0407071v1.

[19] Wayte, R. (2010). A Model of the Electron. Progress in Theoretical Physics.

[20] Osmera, P. (2012). Fractal Dimension of Electron. Proceedings of MENDEL (Conference: MENDEL 2012).

[21] Bowen, D. & Mulkern, R. (2015). An Electron Model Consistent with Electron-Positron Pair Production from High Energy Photons. Journal of Modern Physics, 2015, 6, 1334 –1342.

Appendix 1

In this Appendix, contravariant components of metric tensors are obtained from metrics (21) – (24)

$$\text{I} \quad ds_1^{(+a1)2} = \left(1-\frac{r_6 r}{\rho}\right)c^2dt^2 - \frac{\rho dr^2}{\Delta^{(a)}} - \rho d\theta^2 - \left(r^2+a^2+\frac{r_6 r a^2}{\rho}sin^2\theta\right)sin^2\theta\, d\phi^2 + \frac{2r_6 ra}{\rho}sin^2\theta\, d\phi c dt, \qquad (21)$$

$$\text{H} \quad ds_2^{(+a2)2} = \left(1-\frac{r_6 r}{\rho}\right)c^2dt^2 - \frac{\rho dr^2}{\Delta^{(a)}} - \rho d\theta^2 - \left(r^2+a^2+\frac{r_6 r a^2}{\rho}sin^2\theta\right)sin^2\theta\, d\phi^2 - \frac{2r_6 ra}{\rho}sin^2\theta\, d\phi c dt, \qquad (22)$$

$$\text{V} \quad ds_3^{(+b1)2} = \left(1+\frac{r_6 r}{\rho}\right)c^2dt^2 - \frac{\rho dr^2}{\Delta^{(b)}} - \rho d\theta^2 - \left(r^2+a^2-\frac{r_6 r a^2}{\rho}sin^2\theta\right)sin^2\theta\, d\phi^2 + \frac{2r_6 ra}{\rho}sin^2\theta\, d\phi c dt, \qquad (23)$$

$$\text{H}' \quad ds_4^{(+b2)2} = \left(1+\frac{r_6 r}{\rho}\right)c^2dt^2 - \frac{\rho dr^2}{\Delta^{(b)}} - \rho d\theta^2 - \left(r^2+a^2-\frac{r_6 r a^2}{\rho}sin^2\theta\right)sin^2\theta\, d\phi^2 - \frac{2r_6 ra}{\rho}sin^2\theta\, d\phi c dt; \qquad (24)$$

Calculations were performed using the Symbolic Algebra Library "Sym Py" by Alexander Bindiman.

1) Consider the metric (21)

$$ds_1^{(+a1)2} = \left(1-\frac{r_6 r}{\rho}\right)c^2dt^2 - \frac{\rho dr^2}{\Delta^{(a)}} - \rho d\theta^2 - \left(r^2+a^2+\frac{r_6 r a^2}{\rho}sin^2\theta\right)sin^2\theta\, d\phi^2 + \frac{2r_6 ra}{\rho}sin^2\theta\, d\phi c dt,$$

The covariant components of the metric tensor from this metric are equal to

$$g_{ij}^{(+a1)} = \begin{bmatrix} -\frac{rr_6}{a^2\cos^2(\theta)+r^2}+1 & 0 & 0 & \frac{arr_6\sin^2(\theta)}{a^2\cos^2(\theta)+r^2} \\ 0 & \frac{-a^2\cos^2(\theta)-r^2}{a^2+r^2-rr_6} & 0 & 0 \\ 0 & 0 & -a^2\cos^2(\theta)-r^2 & 0 \\ \frac{arr_6\sin^2(\theta)}{a^2\cos^2(\theta)+r^2} & 0 & 0 & \left(-\frac{a^2rr_6\sin^2(\theta)}{a^2\cos^2(\theta)+r^2}-a^2-r^2\right)\sin^2(\theta) \end{bmatrix}$$

The contravariant components of the metric tensor g_{ij} of a given metric are determined by formulas [8] (57) and (58) $g^{ij} = \frac{\Delta_{ij}}{g}$, where Δ_{ij} is the algebraic complement of the corresponding element of the matrix (g_{ij}), $g = \|g_{ij}\| = -(r^2 + a^2 \cos^2 \theta)^2 \sin^2 \theta$ is the determinant of the matrix (g_{ij}).

As a result of the calculation, we obtain

$$g^{(ij)(+a1)} = \begin{bmatrix} \frac{a^4\cos^2(\theta)+a^2r^2\cos^2(\theta)+a^2r^2+a^2rr_6\sin^2(\theta)+r^4}{a^4\cos^2(\theta)+a^2r^2\cos^2(\theta)+a^2r^2+a^2rr_6\sin^2(\theta)-a^2rr_6+r^4-r^3r_6} & 0 & 0 & \frac{arr_6}{a^4\cos^2(\theta)+a^2r^2\cos^2(\theta)+a^2r^2+a^2rr_6\sin^2(\theta)-a^2rr_6+r^4-r^3r_6} \\ 0 & \frac{-a^2-r^2+rr_6}{a^2\cos^2(\theta)+r^2} & 0 & 0 \\ 0 & 0 & -\frac{1}{a^2\cos^2(\theta)+r^2} & 0 \\ \frac{arr_6}{a^4\cos^2(\theta)+a^2r^2\cos^2(\theta)+a^2r^2+a^2rr_6\sin^2(\theta)-a^2rr_6+r^4-r^3r_6} & 0 & 0 & \frac{-a^2\cos^2(\theta)-r^2+rr_6}{a^4\sin^2(\theta)\cos^2(\theta)+a^2r^2\sin^2(\theta)\cos^2(\theta)+a^2r^2\sin^2(\theta)+a^2rr_6\sin^4(\theta)-a^2rr_6\sin^2(\theta)+r^4\sin^2(\theta)-r^3r_6\sin^2(\theta)} \end{bmatrix}$$

2) Consider the metric (22)

$$ds_2^{(+a2)2} = \left(1 - \frac{r_6 r}{\rho}\right) c^2dt^2 - \frac{\rho dr^2}{\Delta^{(a)}} - \rho d\theta^2 - \left(r^2 + a^2 + \frac{r_6 r a^2}{\rho} \sin^2\theta\right) \sin^2\theta \, d\phi^2 - \frac{2r_6 ra}{\rho} \sin^2\theta \, d\phi c dt,$$

The covariant components of the metric tensor from this metric are equal to

$$\begin{bmatrix} -\frac{rr_6}{a^2\cos^2(\theta)+r^2}+1 & 0 & 0 & -\frac{arr_6\sin^2(\theta)}{a^2\cos^2(\theta)+r^2} \\ 0 & \frac{-a^2\cos^2(\theta)-r^2}{a^2+r^2-rr_6} & 0 & 0 \\ 0 & 0 & -a^2\cos^2(\theta)-r^2 & 0 \\ -\frac{arr_6\sin^2(\theta)}{a^2\cos^2(\theta)+r^2} & 0 & 0 & \left(-\frac{a^2rr_6\sin^2(\theta)}{a^2\cos^2(\theta)+r^2}-a^2-r^2\right)\sin^2(\theta) \end{bmatrix}$$

The contravariant components of the metric tensor g^{ij} of a given metric are equal to

$$\begin{bmatrix} \frac{a^4\cos^2(\theta)+a^2r^2\cos^2(\theta)+a^2r^2+a^2rr_6\sin^2(\theta)+r^4}{a^4\cos^2(\theta)+a^2r^2\cos^2(\theta)+a^2r^2+a^2rr_6\sin^2(\theta)-a^2rr_6+r^4-r^3r_6} & 0 & 0 & -\frac{arr_6}{a^4\cos^2(\theta)+a^2r^2\cos^2(\theta)+a^2r^2+a^2rr_6\sin^2(\theta)-a^2rr_6+r^4-r^3r_6} \\ 0 & \frac{-a^2-r^2+rr_6}{a^2\cos^2(\theta)+r^2} & 0 & 0 \\ 0 & 0 & -\frac{1}{a^2\cos^2(\theta)+r^2} & 0 \\ -\frac{arr_6}{a^4\cos^2(\theta)+a^2r^2\cos^2(\theta)+a^2r^2+a^2rr_6\sin^2(\theta)-a^2rr_6+r^4-r^3r_6} & 0 & 0 & \frac{-a^2\cos^2(\theta)-r^2+rr_6}{a^4\sin^2(\theta)\cos^2(\theta)+a^2r^2\sin^2(\theta)\cos^2(\theta)+a^2r^2\sin^2(\theta)+a^2rr_6\sin^4(\theta)-a^2rr_6\sin^2(\theta)+r^4\sin^2(\theta)-r^3r_6\sin^2(\theta)} \end{bmatrix}$$

2) Consider the metric (23)

$$ds_3^{(+b1)2} = \left(1 + \frac{r_6 r}{\rho}\right) c^2dt^2 - \frac{\rho dr^2}{\Delta^{(b)}} - \rho d\theta^2 - \left(r^2 + a^2 - \frac{r_6 r a^2}{\rho} \sin^2\theta\right) \sin^2\theta \, d\phi^2 + \frac{2r_6 ra}{\rho} \sin^2\theta \, d\phi c dt,$$

The covariant components of the metric tensor from this metric are equal to

$$\begin{bmatrix} \frac{rr_6}{a^2\cos^2(\theta)+r^2}+1 & 0 & 0 & \frac{arr_6\sin^2(\theta)}{a^2\cos^2(\theta)+r^2} \\ 0 & \frac{-a^2\cos^2(\theta)-r^2}{a^2+r^2+rr_6} & 0 & 0 \\ 0 & 0 & -a^2\cos^2(\theta)-r^2 & 0 \\ \frac{arr_6\sin^2(\theta)}{a^2\cos^2(\theta)+r^2} & 0 & 0 & \left(\frac{a^2rr_6\sin^2(\theta)}{a^2\cos^2(\theta)+r^2}-a^2-r^2\right)\sin^2(\theta) \end{bmatrix}$$

The contravariant components of the metric tensor g^{ij} of a given metric are equal to

$$\begin{bmatrix} \frac{a^4\cos^2(\theta)+a^2r^2\cos^2(\theta)+a^2r^2-a^2rr_6\sin^2(\theta)+r^4}{a^4\cos^2(\theta)+a^2r^2\cos^2(\theta)+a^2r^2-a^2rr_6\sin^2(\theta)+a^2rr_6+r^4+r^3r_6} & 0 & 0 & \frac{arr_6}{a^4\cos^2(\theta)+a^2r^2\cos^2(\theta)+a^2r^2-a^2rr_6\sin^2(\theta)+a^2rr_6+r^4+r^3r_6} \\ 0 & \frac{-a^2-r^2-rr_6}{a^2\cos^2(\theta)+r^2} & 0 & 0 \\ 0 & 0 & -\frac{1}{a^2\cos^2(\theta)+r^2} & 0 \\ \frac{arr_6}{a^4\cos^2(\theta)+a^2r^2\cos^2(\theta)+a^2r^2-a^2rr_6\sin^2(\theta)+a^2rr_6+r^4+r^3r_6} & 0 & 0 & \frac{-a^2\cos^2(\theta)-r^2-rr_6}{a^4\sin^2(\theta)\cos^2(\theta)+a^2r^2\sin^2(\theta)\cos^2(\theta)+a^2r^2\sin^2(\theta)-a^2rr_6\sin^4(\theta)+a^2rr_6\sin^2(\theta)+r^4\sin^2(\theta)+r^3r_6\sin^2(\theta)} \end{bmatrix}$$

2) Consider the metric (24)

$$ds_4^{(+b2)2}=\left(1+\frac{r_6 r}{\rho}\right)c^2dt^2-\frac{\rho dr^2}{\Delta^{(b)}}-\rho d\theta^2-\left(r^2+a^2-\frac{r_6 ra^2}{\rho}sin^2\,\theta\right)sin^2\,\theta\,d\phi^2-\frac{2r_6 ra}{\rho}sin^2\,\theta\,d\phi cdt;$$

The covariant components of the metric tensor from this metric are equal to

$$\begin{bmatrix} \frac{rr_6}{a^2\cos^2(\theta)+r^2}+1 & 0 & 0 & -\frac{arr_6\sin^2(\theta)}{a^2\cos^2(\theta)+r^2} \\ 0 & \frac{-a^2\cos^2(\theta)-r^2}{a^2+r^2+rr_6} & 0 & 0 \\ 0 & 0 & -a^2\cos^2(\theta)-r^2 & 0 \\ -\frac{arr_6\sin^2(\theta)}{a^2\cos^2(\theta)+r^2} & 0 & 0 & \left(\frac{a^2rr_6\sin^2(\theta)}{a^2\cos^2(\theta)+r^2}-a^2-r^2\right)\sin^2(\theta) \end{bmatrix}$$

The contravariant components of the metric tensor g^{ij} of a given metric are equal to

$$\begin{bmatrix} \frac{a^4\cos^2(\theta)+a^2r^2\cos^2(\theta)+a^2r^2-a^2rr_6\sin^2(\theta)+r^4}{a^4\cos^2(\theta)+a^2r^2\cos^2(\theta)+a^2r^2-a^2rr_6\sin^2(\theta)+a^2rr_6+r^4+r^3r_6} & 0 & 0 & -\frac{arr_6}{a^4\cos^2(\theta)+a^2r^2\cos^2(\theta)+a^2r^2-a^2rr_6\sin^2(\theta)+a^2rr_6+r^4+r^3r_6} \\ 0 & \frac{-a^2-r^2-rr_6}{a^2\cos^2(\theta)+r^2} & 0 & 0 \\ 0 & 0 & -\frac{1}{a^2\cos^2(\theta)+r^2} & 0 \\ -\frac{arr_6}{a^4\cos^2(\theta)+a^2r^2\cos^2(\theta)+a^2r^2-a^2rr_6\sin^2(\theta)+a^2rr_6+r^4+r^3r_6} & 0 & 0 & \frac{-a^2\cos^2(\theta)-r^2-rr_6}{a^4\sin^2(\theta)\cos^2(\theta)+a^2r^2\sin^2(\theta)\cos^2(\theta)+a^2r^2\sin^2(\theta)-a^2rr_6\sin^4(\theta)+a^2rr_6\sin^2(\theta)+r^4\sin^2(\theta)+r^3r_6\sin^2(\theta)} \end{bmatrix}$$